ANALYSIS OF A DISCONTINUOUS GALERKIN METHOD FOR ELASTODYNAMIC EQUATIONS. APPLICATION TO 3D WAVE PROPAGATION.

Sarah Delcourte, Nathalie Glinsky

ANALYSIS OF A DISCONTINUOUS GALERKIN METHOD FOR ELASTODYNAMIC EQUATIONS. APPLICATION TO 3D WAVE PROPAGATION.

SARAH DELCOURTE

Université de Lyon, CNRS UMR5208, Université Lyon 1, Institut Camille Jordan,
43 blvd du 11 novembre 1918, F-69622 Villeurbanne Cedex, France.

NATHALIE GLINSKY

IFSTTAR/CETE Méditerranée, 56 boulevard Stalingrad, 06359 Nice cedex 4, France.
INRIA Sophia Antipolis Méditerranée, 2004 route des Lucioles, 06902 Sophia Antipolis Cedex, France.

Abstract

In this paper, we introduce a second-order leap-frog time scheme combined with a high-order discontinuous Galerkin method for the solution of the 3D elastodynamic equations. We prove that this explicit scheme is stable under a CFL type condition obtained from a discrete energy which is preserved in domains with free surface or decreasing in domains with absorbing boundary conditions. Moreover, we study the convergence of the method for both the semi-discrete and the fully discrete scheme, and we illustrate the convergence results by the propagation of an eigenmode. Finally, we examine a more realistic 3D test case simulating the propagation of the wave produced by an explosive source in a half-space which constitutes a validation of the source introduction and the absorbing boundary conditions.

AMS subject classifications: 35L50,35F10,35F15,35L05,35Q99

Key words: discontinuous Galerkin method, centered flux, leap-frog scheme, elastodynamic equation

1 Introduction

In the last few decades, the computational seismology has become an essential tool to simulate realistic wavefields of local, regional or even global wave propagation problems. The physics governing these phenomena is now well understood and many different accurate numerical methods have been developed and can deal with three-dimensional realistic applications thanks to a continuous increase of the computational resources and the use of parallel computational facilities.

Among all the numerical methods proposed for simulations in time domain, the most popular is undoubtedly the finite difference (FD) method and its many improvements from the initial FD schemes proposed by Alterman and Karal [3] or Kelly et al. [19] such as, for instance, the introduction of the velocity-stress system and the staggered-grids (Madariaga [23], Virieux [31]), fourth-order schemes in space (Bayliss et al. [5], Levander [21]) and rotated staggered-grids (Saenger et al. [29]) allowing strong fluctuations of the elastic parameters. Their major drawback is the restriction to cartesian grids not suited for geometrical internal or surfacic nonlinearities (topography) but, the use of non uniform grids (Pitarka [26]) or even discontinuous grids (Aoi and Fujiwara [2]) enabled improving the accuracy at the free surface and, more recently, an hybrid method coupling a finite-difference technique for the most part of the domain and a finite-element method in subdomains containing the nonlinearities (topography, faults) has been proposed (Moczo et al. [25], Galis et al. [14]). Some other methods have been further developed such as finite element (FE) methods which allow meshes adapted to complex geometries [22], [24], [4]. However, they are very costly because one needs to invert a global mass matrix at each time step. This difficulty was overcome by the use of Gauss-Lobato Legendre quadrature formulae at the root of the spectral element methods (SEM) which have been widely applied to quadrangular and hexaedral meshes (see, for instance [20, 9] amongst many contributions). Note the recent development of two non conforming discontinuous Galerkin spectral element methods and their convergence and stability analysis for the wave propagation in 2D quadrangular meshes [1] and 3D affine hexahedral meshes [30]. In very complex media, the use of simplicial meshes permits a better approximation of the geometry

(bann, topography, faults). For this reason, we study a high-order Discontinuous Galerkin (DG) method applied to tetrahedral meshes.

The Discontinuous Galerkin (DG) method has been initially introduced by Reed and Hill [27] for the solution of neutron transport problems. Neglected during twenty years, it became very popular to solve hyperbolic problems especially computational electromagnetics [13]. In spite of its success in many domains of applications, this method has been rarely applied to seismic wave propagation problems. Käeser et al. (see [18, 12] and references therein) proposed a DG finite element scheme that uses the ADER approach based on an upwind scheme in order to solve the elastic wave equations with the same high accuracy in both space and time. However, despite its accuracy, this scheme is diffusive; it is the reason why we propose another combination which preserves a discrete elastodynamic energy.

In this paper, we study the P-SV seismic wave propagation considering an isotropic, linearly elastic medium by solving the velocity-stress formulation of the elastodynamic equations. For the discretization of this system, we focus on a DG method which is a finite element method allowing discontinuities at the interfaces introduced via numerical fluxes as for finite volumes. Our method is based on centered fluxes and a leap-frog time-discretization which lead to a non-dissipative combination [11]. Moreover, the method is suitable for complex unstructured simplicial meshes. The extension to higher order in space is realized by Lagrange polynomial functions (of degree 0 to 3 for our solver), defined locally on tetrahedra and do not necessitate the inversion of a global mass matrix since an explicit time scheme is used.

This article is organized as follows. In section 2, we state the velocity-stress formulation in a symmetrical pseudo-conservative form. Then, in section 3, we detail the discretization of the equations system by the Discontinuous Galerkin method based on centered fluxes in space, combined with a leap-frog scheme in time. The approximation of the boundary conditions is also presented. After, we study, in section 4, the preservation of a discrete elastodynamic energy and the stability of the scheme, taking into account the free surface or the absorbing boundary conditions. Section 5 is devoted to the convergence analysis of the semi-discrete and fully discretized schemes. Finally, we illustrate this study in section 6 by some numerical results in three dimensions of space: the propagation of an eigenmode and the case of an explosive source in a half-space.

2 Velocity-stress formulation in pseudo-conservative form

The P-SV wave propagation in an isotropic, linearly elastic medium is modelised by the elastodynamic equations, which initially write in displacement-stress formulation; let be $\vec{U} = (U_\alpha)_{\alpha\in\{x,y,z\}}$ the displacement vector and $\overline{\overline{\sigma}} = (\sigma_{\alpha,\beta})_{\alpha,\beta\in\{x,y,z\}}$, the stress tensor, then the system reads

$$\left\{\begin{array}{rcl} \rho\ \partial_t^2\vec{U} &=& \nabla\cdot\overline{\overline{\sigma}}\,, \\ \overline{\overline{\sigma}} &=& \lambda\ (\nabla\cdot\vec{U})\ \overline{\overline{I}} + \mu\ (\boldsymbol{\nabla}\vec{U} + (\boldsymbol{\nabla}\vec{U})^t)\,, \end{array}\right. \tag{1}$$

where $\overline{\overline{I}}$ is the identity matrix, ρ is the density of the medium and λ and μ are the Lamé parameters related to shear and compressional velocities (v_s and v_p) in the medium by $v_s = \sqrt{\frac{\mu}{\rho}}$ and $v_p = \sqrt{\frac{\lambda+2\mu}{\rho}}$.

We introduce the velocity vector $\vec{V} = \partial_t\vec{U}$ in the equation (1) and obtain the first-order velocity-stress formulation [31]:

$$\left\{\begin{array}{rcl} \rho\ \partial_t\vec{V} &=& \nabla\cdot\overline{\overline{\sigma}}\,, \\ \partial_t\overline{\overline{\sigma}} &=& \lambda\ (\nabla\cdot\vec{V})\ \overline{\overline{I}} + \mu\ (\boldsymbol{\nabla}\vec{V} + (\boldsymbol{\nabla}\vec{V})^t)\,. \end{array}\right. \tag{2}$$

Let $\vec{W} = \left(\vec{V}, \vec{\sigma}\right)^t$ be the vector composed of the velocity components $\vec{V} = (V_x, V_y, V_z)^t$ and the stress components $\vec{\sigma} = (\sigma_{xx}, \sigma_{yy}, \sigma_{zz}, \sigma_{xy}, \sigma_{xz}, \sigma_{yz})^t$, since the stress tensor is symmetrical, then, the system (2) can be rewritten as

$$\partial_t\vec{W} + \sum_{\alpha\in\{x,y,z\}} A_\alpha\,(\rho,\lambda,\mu)\ \ \partial_\alpha\vec{W} = 0\,. \tag{3}$$

We choose here not to detail the matrices $A_\alpha\,(\rho,\lambda,\mu)$.

In order to express the system (3) in a pseudo conservative form, we introduce the following change of variables on the stress components,

$$\vec{\tilde{\sigma}} = \mathbb{T}\,\vec{\sigma} = \left(\frac{\sigma_{xx}+\sigma_{yy}+\sigma_{zz}}{3}, \frac{2\sigma_{xx}-\sigma_{yy}-\sigma_{zz}}{3}, \frac{-\sigma_{xx}+2\sigma_{yy}-\sigma_{zz}}{3}, \sigma_{xy}, \sigma_{xz}, \sigma_{yz} \right). \tag{4}$$

So, the system reads

$$\left\{ \begin{array}{r} \rho\ \partial_t \vec{V} = \displaystyle\sum_{\alpha\in\{x,y,z\}} \mathbb{M}_\alpha\ \partial_\alpha \vec{\tilde{\sigma}}\,, \\ \Lambda_0(\lambda,\mu)\ \partial_t \vec{\tilde{\sigma}} = \displaystyle\sum_{\alpha\in\{x,y,z\}} \mathbb{N}_\alpha\ \partial_\alpha \vec{V}\,, \end{array} \right. \tag{5}$$

where $\Lambda_0(\lambda,\mu) = diag\left(\frac{3}{3\lambda+2\mu}, \frac{3}{2\mu}, \frac{3}{2\mu}, \frac{1}{\mu}, \frac{1}{\mu}, \frac{1}{\mu}\right)$ is a diagonal matrix containing the characteristics of the medium and

$$\mathbb{M}_x = \begin{pmatrix} 1 & 1 & 0 & 0 & 0 & 0 \\ 0 & 0 & 0 & 1 & 0 & 0 \\ 0 & 0 & 0 & 0 & 1 & 0 \end{pmatrix}, \mathbb{M}_y = \begin{pmatrix} 0 & 0 & 0 & 1 & 0 & 0 \\ 1 & 0 & 1 & 0 & 0 & 0 \\ 0 & 0 & 0 & 0 & 0 & 1 \end{pmatrix}, \mathbb{M}_z = \begin{pmatrix} 0 & 0 & 0 & 0 & 1 & 0 \\ 0 & 0 & 0 & 0 & 0 & 1 \\ 1 & -1 & -1 & 0 & 0 & 0 \end{pmatrix},$$

$$\mathbb{N}_x = \begin{pmatrix} 1 & 0 & 0 \\ 2 & 0 & 0 \\ -1 & 0 & 0 \\ 0 & 1 & 0 \\ 0 & 0 & 1 \\ 0 & 0 & 0 \end{pmatrix}, \mathbb{N}_y = \begin{pmatrix} 0 & 1 & 0 \\ 0 & -1 & 0 \\ 0 & 2 & 0 \\ 1 & 0 & 0 \\ 0 & 0 & 0 \\ 0 & 0 & 1 \end{pmatrix}, \mathbb{N}_z = \begin{pmatrix} 0 & 0 & 1 \\ 0 & 0 & -1 \\ 0 & 0 & -1 \\ 0 & 0 & 0 \\ 1 & 0 & 0 \\ 0 & 1 & 0 \end{pmatrix}.$$

We can notice that now the matrices $\mathbb{M}_\alpha$ and $\mathbb{N}_\alpha$ ($\alpha = x, y, z$) are constant and do not depend anymore on the material properties. So, the system (5) is a pseudo-conservative formulation of (3). At last, we multiply the second equation of (5) by the following positive definite symmetrical (PDS) matrix

$$\mathbb{S} = \begin{pmatrix} 1 & 0 & 0 & 0 & 0 & 0 \\ 0 & \frac{2}{3} & \frac{1}{3} & 0 & 0 & 0 \\ 0 & \frac{1}{3} & \frac{2}{3} & 0 & 0 & 0 \\ 0 & 0 & 0 & 1 & 0 & 0 \\ 0 & 0 & 0 & 0 & 1 & 0 \\ 0 & 0 & 0 & 0 & 0 & 1 \end{pmatrix}$$

in order to obtain a symmetrical system. Therefore, we finally get the symmetrical pseudo-conservative formulation:

$$\left\{ \begin{array}{r} \rho\partial_t \vec{V} = \displaystyle\sum_{\alpha\in\{x,y,z\}} \mathbb{M}_\alpha \partial_\alpha \vec{\tilde{\sigma}}\,, \\ \Lambda(\lambda,\mu)\partial_t \vec{\tilde{\sigma}} = \displaystyle\sum_{\alpha\in\{x,y,z\}} \mathbb{M}_\alpha^t \partial_\alpha \vec{V}\,, \end{array} \right. \tag{6}$$

where $\Lambda(\lambda,\mu) = \mathbb{S}\Lambda_0(\lambda,\mu)$ is a positive definite symmetrical matrix whose spectrum is

$$Sp\{\Lambda\} = \left\{ \frac{1}{2\mu}, \frac{3}{2\mu}, \frac{1}{\mu}, \frac{1}{\mu}, \frac{1}{\mu}, \frac{3}{3\lambda+2\mu} \right\} \subset \mathbb{R}_+^*$$

and we can notice that $\mathbb{S}\mathbb{N}_\alpha = \mathbb{M}_\alpha^t$ ($\alpha = x, y, z$). This formulation will be very useful to establish the energy preservation. Then, we add:

(i) a physical boundary condition on the free surface

$$\overline{\overline{\sigma}}\,\vec{\mathbf{n}} = \vec{0}, \tag{7}$$

which will be rewritten by respect to $\vec{\tilde{\sigma}}$ in section 3.3.

(ii) absorbing boundary conditions

$$\mathbb{P}\vec{\vec{\sigma}} = -\mathbb{A}\vec{V} \quad \text{and} \quad \mathbb{P}^t\vec{V} = -\mathbb{B}\vec{\vec{\sigma}}, \tag{8}$$

(where the matrices $\mathbb{P}$, $\mathbb{A}$ and $\mathbb{B}$ will be specified in section 3.3) to approximate an infinite domain.

At last, we need to impose initial data

$$\vec{V}(0) = \vec{V}_0 \quad \text{and} \quad \vec{\vec{\sigma}}(0) = \vec{\vec{\sigma}}_0, \tag{9}$$

to ensure the existence and the uniqueness of the solution $(\vec{V}, \vec{\vec{\sigma}})$ of the system (6)-(7)-(8)-(9).

3 A discontinuous Galerkin method combined with a leap-frog scheme

3.1 Integration on a simplex

We consider a bounded polyhedral domain Ω of $\mathbb{R}^3$, discretized in N_T tetrahedra $\mathcal{T}_i$, which form a partition of the domain. We assume that the characteristics of the medium are constant over each element $\mathcal{T}_i$ and denoted by $(\rho_i, \lambda_i, \mu_i)$. We multiply, in the sense of the scalar product, the first (resp. the second) equation of the problem (6) by a vector field $\vec{\varphi}_i \in \mathbb{R}^3$ (resp. $\vec{\psi}_i \in \mathbb{R}^6$) and we integrate them on each element $\mathcal{T}_i$. Then, we apply the Green formula to the right-hand sides:

$$\rho_i \int_{\mathcal{T}_i} \vec{\varphi}_i^t \partial_t \vec{V} dv = \sum_{\alpha\in\{x,y,z\}} \left[-\int_{\mathcal{T}_i} (\partial_\alpha \vec{\varphi}_i)^t \mathbb{M}_\alpha \vec{\vec{\sigma}} dv + \int_{\partial\mathcal{T}_i} \vec{\varphi}_i^t \mathbb{M}_\alpha \vec{\vec{\sigma}} n_{\alpha_i} ds \right], \tag{10a}$$

$$\int_{\mathcal{T}_i} \vec{\psi}_i^t \Lambda_i \partial_t \vec{\vec{\sigma}} dv = \sum_{\alpha\in\{x,y,z\}} \left[-\int_{\mathcal{T}_i} (\partial_\alpha \vec{\psi}_i)^t \mathbb{M}_\alpha^t \vec{V} dv + \int_{\partial\mathcal{T}_i} \vec{\psi}_i^t \mathbb{M}_\alpha^t \vec{V} n_{\alpha_i} ds \right], \tag{10b}$$

where we set $\Lambda_i = \Lambda(\lambda_i, \mu_i)$ and $\vec{\mathbf{n}}_i = (n_{x_i}, n_{y_i}, n_{z_i})^t$ represents the outwards unit normal vector to $\mathcal{T}_i$.

3.2 Evaluation of volume integrals

The approximations of $\vec{V}$ and $\vec{\vec{\sigma}}$ are denoted by the fields $\vec{V}_h$ and $\vec{\vec{\sigma}}_h$ which are defined locally on each element $\mathcal{T}_i$ and may be discontinuous through the interfaces, so that we set

$$\forall i,\ \vec{V}_{h_{|\mathcal{T}_i}} = \vec{V}_i \quad \text{and} \quad \vec{\vec{\sigma}}_{h_{|\mathcal{T}_i}} = \vec{\vec{\sigma}}_i. \tag{11}$$

Consider the Lagrange nodal interpolants $\varphi_{ij}, \psi_{ij} \in \mathcal{P}_m(\mathcal{T}_i)$, set of polynomials over $\mathcal{T}_i$ with a degree m, then we can write $\vec{V}_i$ and $\vec{\vec{\sigma}}_i$ as linear combinations of time-dependent fields:

$$\vec{V}_i(x,y,z,t) = \sum_{j=1}^{dof} \vec{V}_{ij}(t)\ \varphi_{ij}(x,y,z), \tag{12}$$

$$\vec{\vec{\sigma}}_i(x,y,z,t) = \sum_{j=1}^{dof} \vec{\vec{\sigma}}_{ij}(t)\ \psi_{ij}(x,y,z), \tag{13}$$

where dof denotes the number of degrees of freedom on the element $\mathcal{T}_i$. To approximate the volume integrals on $\mathcal{T}_i$, we just have to replace the fields $\vec{V}$ and $\vec{\vec{\sigma}}$ in (10) by $\vec{V}_h$ and $\vec{\vec{\sigma}}_h$.

3.3 Approximation on faces

To calculate the integrals on $\partial\mathcal{T}_i$ of (10), we split this boundary in internal and boundary faces. We denote by $\mathcal{V}(i)$ the set of indices of the neighboring elements of $\mathcal{T}_i$ and we note by S_{ik} each internal face common to both elements $\mathcal{T}_i$ and $\mathcal{T}_k$, i.e. $S_{ik} = \mathcal{T}_i \cap \mathcal{T}_k$. Moreover, some elements $\mathcal{T}_i$ have one or more faces common to the boundary of the domain. The set of the indices k of such faces $S_{ik} = \mathcal{T}_i \cap \partial\Omega$ is denoted by $\mathcal{E}(i)$ for absorbing boundaries and $\mathcal{K}(i)$

for free surface boundaries. Remark that, for most elements, $\mathcal{E}(i)$ and $\mathcal{K}(i)$ are empty sets. Therefore, introducing $\mathbb{P}_{ik} = \sum_{\alpha\in\{x,y,z\}} \mathbb{M}_\alpha n_{\alpha_{ik}}$, we have:

$$\sum_{\alpha\in\{x,y,z\}} \int_{\partial\mathcal{T}_i} \vec{\varphi}_i^t \mathbb{M}_\alpha \vec{\bar{\sigma}} n_{\alpha_i} ds = \sum_{k\in\mathcal{V}(i)} \int_{S_{ik}} \vec{\varphi}_i^t \mathbb{P}_{ik} \vec{\bar{\sigma}} ds + \sum_{k\in\mathcal{E}(i)} \int_{S_{ik}} \vec{\varphi}_i^t \mathbb{P}_{ik} \vec{\bar{\sigma}} ds + \sum_{k\in\mathcal{K}(i)} \int_{S_{ik}} \vec{\varphi}_i^t \mathbb{P}_{ik} \vec{\bar{\sigma}} ds\,, \quad (14a)$$

$$\sum_{\alpha\in\{x,y,z\}} \int_{\partial\mathcal{T}_i} \vec{\psi}_i^t \mathbb{M}_\alpha^t \vec{V} n_{\alpha_i} ds = \sum_{k\in\mathcal{V}(i)} \int_{S_{ik}} \vec{\psi}_i^t \mathbb{P}_{ik}^t \vec{V} ds + \sum_{k\in\mathcal{E}(i)} \int_{S_{ik}} \vec{\psi}_i^t \mathbb{P}_{ik}^t \vec{V} ds + \sum_{k\in\mathcal{K}(i)} \int_{S_{ik}} \vec{\psi}_i^t \mathbb{P}_{ik}^t \vec{V} ds\,, \quad (14b)$$

where $\vec{\mathbf{n}}_{ik} = (n_{x_{ik}}, n_{y_{ik}}, n_{z_{ik}})^t$ represents the unit normal vector of S_{ik}, oriented from $\mathcal{T}_i$ towards $\mathcal{T}_k$.

For the **interior faces** S_{ik} of $\mathcal{T}_i$ ($k \in \mathcal{V}(i)$), we choose to apply centered fluxes by introducing the mean-value on this face:

$$\vec{V}_{|_{S_{ik}}} \simeq \frac{1}{2}\left(\vec{V}_i + \vec{V}_k\right) \quad \text{and} \quad \vec{\bar{\sigma}}_{|_{S_{ik}}} \simeq \frac{1}{2}\left(\vec{\bar{\sigma}}_i + \vec{\bar{\sigma}}_k\right). \quad (15)$$

For the boundary integrals, two types of boundary conditions have been considered : a free surface condition at the physical interface between air and the medium, and an absorbing condition on the artificial boundaries of an infinite domain.

Free surfaces: On these faces, we compute the fluxes by introducing weakly the physical condition (7) in the third term of (14a) and the physical condition is rewritten in the new variable $\vec{\bar{\sigma}}$ via the change of variables (4). No physical condition is applied to the velocity in the third term of (14b). So, for a boundary face S_{ik} of $\mathcal{T}_i$, with $k \in \mathcal{K}(i)$, this condition reduces to:

$$\vec{V}_{|_{S_{ik}}} \simeq \vec{V}_i \quad \text{and} \quad \mathbb{P}_{ik}\vec{\bar{\sigma}}_{|_{S_{ik}}} = \vec{0}\,. \quad (16)$$

Absorbing surfaces: To simulate infinite domains, we introduce artificial boundaries, on which we impose absorbing conditions. Therefore, for any $k \in \mathcal{E}(i)$ and any real unit vector $\vec{\mathbf{n}}_{ik}$, we define the matrix

$$\mathcal{A}_{n_{ik}}(\rho_i,\lambda_i,\mu_i) = \sum_{\alpha\in\{x,y,z\}} A_\alpha(\rho_i,\lambda_i,\mu_i)\; n_{\alpha_{ik}} = -\begin{pmatrix} 0_{\mathbb{R}^{3\times3}} & \dfrac{1}{\rho_i}\mathbb{P}_{ik} \\ \Lambda_i^{-1}\mathbb{P}_{ik}^t & 0_{\mathbb{R}^{6\times6}} \end{pmatrix}, \quad (17)$$

which is diagonalizable in $\mathbb{R}$, i.e. all its eigenvalues e_k (k=1,...,9) are real:

$$e_1 = -v_{p_i}, \quad e_2 = e_3 = -v_{s_i}, \quad e_4 = e_5 = e_6 = 0, \quad e_7 = e_8 = v_{s_i}, \quad e_9 = v_{p_i}\,,$$

with

$$v_{p_i} = v_p(\rho_i,\lambda_i,\mu_i) = \sqrt{\frac{\lambda_i+2\mu_i}{\rho_i}} \quad \text{and} \quad v_{s_i} = v_s(\rho_i,\lambda_i,\mu_i) = \sqrt{\frac{\mu_i}{\rho_i}} \quad (18)$$

and we note by $\mathcal{P}_n(\rho,\lambda,\mu)$ the matrix whose column k is the right eigenvector associated to the eigenvalue e_k:

$$\begin{pmatrix}
3v_pn_x & -v_sn_xn_y & v_sn_{0,1,-1} & 0 & 0 & 0 & -v_sn_{0,1,-1} & v_sn_xn_y & -3v_pn_x \\
3v_pn_y & v_sn_{1,0,-1} & -v_sn_xn_y & 0 & 0 & 0 & v_sn_xn_y & -v_sn_{1,0,-1} & -3v_pn_y \\
3v_pn_z & v_sn_yn_z & v_sn_xn_z & 0 & 0 & 0 & -v_sn_xn_z & -v_sn_yn_z & -3v_pn_z \\
3\lambda+2\mu & 0 & 0 & -n_xn_{0,1,1} & -n_yn_{1,0,1} & -n_zn_{1,1,0} & 0 & 0 & 3\lambda+2\mu \\
2\mu n_{2,-1,-1} & -2\mu n_x^2n_y & 2\mu n_xn_{0,1,-1} & n_xn_{0,1,1} & n_yn_{1,0,-2} & n_zn_{1,-2,0} & 2\mu n_xn_{0,1,-1} & -2\mu n_x^2n_y & 2\mu n_{2,-1,-1} \\
-2\mu n_{1,-2,1} & 2\mu n_yn_{1,0,-1} & -2\mu n_xn_y^2 & n_xn_{0,1,-2} & n_yn_{1,0,1} & n_zn_{-2,1,0} & -2\mu n_xn_y^2 & 2\mu n_yn_{1,0,-1} & -2\mu n_{1,-2,1} \\
6\mu n_xn_y & \mu n_xn_{1,-1,-1} & \mu n_yn_{-1,1,-1} & 0 & 0 & 3n_xn_yn_z & \mu n_yn_{-1,1,-1} & \mu n_xn_{1,-1,-1} & 6\mu n_xn_y \\
6\mu n_xn_z & 0 & \mu n_zn_{1,1,-1} & 0 & 3n_xn_yn_z & 0 & \mu n_zn_{1,1,-1} & 0 & 6\mu n_xn_z \\
6\mu n_yn_z & \mu n_zn_{1,1,-1} & 0 & 3n_xn_yn_z & 0 & 0 & 0 & \mu n_zn_{1,1,-1} & 6\mu n_yn_z
\end{pmatrix}$$

where, to simplify, we set $n_{a,b,c} = an_x^2 + bn_y^2 + cn_z^2$. Then, the boundary absorbing conditions consist in an upwind technique where we only take into account the outgoing waves neglecting the ingoing waves part. For that, we approximate $\mathcal{A}_{n_{ik}}$ by the matrix $\mathcal{A}^+_{n_{ik}}$ where we set $\mathcal{A}^+_{n_{ik}} = \left(\mathcal{P}_{n_{ik}}\mathcal{D}^+\mathcal{P}^{-1}_{n_{ik}}\right)(\rho_i,\lambda_i,\mu_i)$ with $\mathcal{D}^+(\rho_i,\lambda_i,\mu_i)$ the diagonal matrix composed by the positive eigenvalues of $\mathcal{A}_{n_{ik}}$. Therefore, according to (17), we have to approximate

$$\begin{pmatrix} \mathbb{P}_{ik}\vec{\bar{\sigma}} \\ \mathbb{P}_{ik}^t\vec{V} \end{pmatrix} = -\begin{pmatrix} \rho_i\overline{\overline{I}}_3 & 0_{\mathbb{R}^{3\times6}} \\ 0_{\mathbb{R}^{6\times3}} & \Lambda_i \end{pmatrix} \mathcal{A}_{n_{ik}}(\rho_i,\lambda_i,\mu_i) \begin{pmatrix} \vec{V} \\ \vec{\bar{\sigma}} \end{pmatrix}, \quad (19)$$

where $\overline{\overline{I}}_3$ denotes the identity matrix, by

$$\begin{pmatrix} \mathbb{P}_{ik}\vec{\vec{\sigma}} \\ \mathbb{P}_{ik}^t\vec{V} \end{pmatrix} \simeq -\begin{pmatrix} \rho_i\overline{\overline{I}}_3 & 0_{\mathbb{R}^{3\times 6}} \\ 0_{\mathbb{R}^{6\times 3}} & \Lambda_i \end{pmatrix} \mathcal{A}^+_{n_{ik}}(\rho_i,\lambda_i,\mu_i) \begin{pmatrix} \vec{V}_i \\ \vec{\vec{\sigma}}_i \end{pmatrix}. \tag{20}$$

After calculus, we obtain:

$$\begin{pmatrix} \rho_i\overline{\overline{I}}_3 & 0_{\mathbb{R}^{3\times 6}} \\ 0_{\mathbb{R}^{6\times 3}} & \Lambda_i \end{pmatrix} \mathcal{A}^+_{n_{ik}}(\rho_i,\lambda_i,\mu_i) = \frac{1}{2}\begin{pmatrix} \mathbb{A}_{ik} & -\mathbb{P}_{ik} \\ -\mathbb{P}_{ik}^t & \mathbb{B}_{ik} \end{pmatrix} \tag{21}$$

where

$$\mathbb{A}_{ik} = \rho_i \begin{pmatrix} (v_{p_i}-v_{s_i})n_{x_{ik}}^2 + v_{s_i} & (v_{p_i}-v_{s_i})n_{x_{ik}}n_{y_{ik}} & (v_{p_i}-v_{s_i})n_{x_{ik}}n_{z_{ik}} \\ (v_{p_i}-v_{s_i})n_{x_{ik}}n_{y_{ik}} & (v_{p_i}-v_{s_i})n_{y_{ik}}^2 + v_{s_i} & (v_{p_i}-v_{s_i})n_{y_{ik}}n_{z_{ik}} \\ (v_{p_i}-v_{s_i})n_{x_{ik}}n_{z_{ik}} & (v_{p_i}-v_{s_i})n_{y_{ik}}n_{z_{ik}} & (v_{p_i}-v_{s_i})n_{z_{ik}}^2 + v_{s_i} \end{pmatrix} \tag{22}$$

and

$$\begin{aligned} \mathbb{B}_{ik} \;=\; & \frac{1}{\rho_i v_{s_i}} \begin{pmatrix} 1 & n_{x_{ik}}^2 - n_{z_{ik}}^2 & n_{y_{ik}}^2 - n_{z_{ik}}^2 & 2n_{x_{ik}}n_{y_{ik}} & 2n_{x_{ik}}n_{z_{ik}} & 2n_{y_{ik}}n_{z_{ik}} \\ n_{x_{ik}}^2 - n_{z_{ik}}^2 & n_{x_{ik}}^2 + n_{z_{ik}}^2 & n_{z_{ik}}^2 & n_{x_{ik}}n_{y_{ik}} & 0 & -n_{y_{ik}}n_{z_{ik}} \\ n_{y_{ik}}^2 - n_{z_{ik}}^2 & n_{z_{ik}}^2 & n_{y_{ik}}^2 + n_{z_{ik}}^2 & n_{x_{ik}}n_{y_{ik}} & -n_{x_{ik}}n_{z_{ik}} & 0 \\ 2n_{x_{ik}}n_{y_{ik}} & n_{x_{ik}}n_{y_{ik}} & n_{x_{ik}}n_{y_{ik}} & n_{x_{ik}}^2 + n_{y_{ik}}^2 & n_{y_{ik}}n_{z_{ik}} & n_{x_{ik}}n_{z_{ik}} \\ 2n_{x_{ik}}n_{z_{ik}} & 0 & -n_{x_{ik}}n_{z_{ik}} & n_{y_{ik}}n_{z_{ik}} & n_{x_{ik}}^2 + n_{z_{ik}}^2 & n_{x_{ik}}n_{y_{ik}} \\ 2n_{y_{ik}}n_{z_{ik}} & -n_{y_{ik}}n_{z_{ik}} & 0 & n_{x_{ik}}n_{z_{ik}} & n_{x_{ik}}n_{y_{ik}} & n_{y_{ik}}^2 + n_{z_{ik}}^2 \end{pmatrix} \\ & + \frac{v_{s_i}-v_{p_i}}{\rho_i v_{p_i} v_{s_i}} \begin{pmatrix} 1 \\ n_{x_{ik}}^2 - n_{z_{ik}}^2 \\ n_{y_{ik}}^2 - n_{z_{ik}}^2 \\ 2n_{x_{ik}}n_{y_{ik}} \\ 2n_{x_{ik}}n_{z_{ik}} \\ 2n_{y_{ik}}n_{z_{ik}} \end{pmatrix} \otimes \begin{pmatrix} 1 \\ n_{x_{ik}}^2 - n_{z_{ik}}^2 \\ n_{y_{ik}}^2 - n_{z_{ik}}^2 \\ 2n_{x_{ik}}n_{y_{ik}} \\ 2n_{x_{ik}}n_{z_{ik}} \\ 2n_{y_{ik}}n_{z_{ik}} \end{pmatrix}. \end{aligned} \tag{23}$$

Finally, for a boundary face S_{ik} of $\mathcal{T}_i$ with $k \in \mathcal{E}(i)$, the fluxes are approximated in (14) by:

$$\int_{S_{ik}} \vec{\varphi}_i^t \mathbb{P}_{ik}\vec{\vec{\sigma}}\; ds \;\simeq\; \int_{S_{ik}} \frac{\vec{\varphi}_i^t}{2}\left[-\mathbb{A}_{ik}\;\vec{V}_i + \mathbb{P}_{ik}\;\vec{\vec{\sigma}}_i\right] ds\,, \tag{24}$$

$$\int_{S_{ik}} \vec{\psi}_i^t \mathbb{P}_{ik}^t\vec{V}\; ds \;\simeq\; \int_{S_{ik}} \frac{\vec{\psi}_i^t}{2}\left[\mathbb{P}_{ik}^t\;\vec{V}_i - \mathbb{B}_{ik}\;\vec{\vec{\sigma}}_i\right] ds\,. \tag{25}$$

Remark 1 *The absorbing boundary conditions (8) follow from (20)-(21). It is a first-order approximation, efficient for waves with a normal incidence to the artificial boundaries but whose accuracy could be improved especially to limit reflections in presence of grazing waves.*

Remark 2 $\mathbb{A}_{ik}$ *is a symmetrical positive definite matrix whose spectrum is*

$$Sp(\mathbb{A}_{ik}) = \{\rho_i v_{p_i}, \rho_i v_{s_i}, \rho_i v_{s_i}\}\,,$$

whereas $\mathbb{B}_{ik}$ *is a symmetrical semi-definite positive matrix. Indeed, we have*

$$det(\mathbb{B}_{ik} - x\overline{\overline{I}}_6) = x^3(ax^3 + bx^2 + cx + d)$$

where

$$a = 1,$$

$$b = -\frac{1}{\rho_i v_{p_i} v_{s_i}}\left[v_{p_i}(2 - 2n_{y_{ik}}^2 + n_{z_{ik}}^2 - n_{z_{ik}}^4 + 2n_{y_{ik}}^4 + 2n_{y_{ik}}^2 n_{z_{ik}}^2) + v_{s_i}(2 + n_{z_{ik}}^4 - 2n_{y_{ik}}^4 + 2n_{y_{ik}}^2 - 2n_{y_{ik}}^2 n_{z_{ik}}^2)\right],$$

$$\begin{aligned} c = \frac{1}{\rho_i^2 v_{p_i} v_{s_i}^2} \quad & \left[v_{p_i}(1 + 2n_{y_{ik}}^4 - 2n_{y_{ik}}^2 - n_{z_{ik}}^4 + n_{z_{ik}}^2 - n_{y_{ik}}^2 n_{z_{ik}}^2 + 3n_{y_{ik}}^2 n_{z_{ik}}^4 + 3n_{y_{ik}}^4 n_{z_{ik}}^2)\right. \\ & \left. + v_{s_i}(4 - n_{y_{ik}}^2 + n_{y_{ik}}^4 + 2n_{y_{ik}}^2 + 4n_{y_{ik}}^2 n_{z_{ik}}^2 - 3n_{y_{ik}}^2 n_{z_{ik}}^4 - 3n_{y_{ik}}^4 n_{z_{ik}}^2 + 3n_{y_{ik}}^4 n_{z_{ik}}^2)\right], \end{aligned}$$

$$d = -\frac{1}{\rho_i^3 v_{p_i} v_{s_i}^2}\left(2 + 2n_{z_{ik}}^2 - 3n_{y_{ik}}^2 + 3n_{y_{ik}}^4 - n_{z_{ik}}^4 - n_{y_{ik}}^2 n_{z_{ik}}^2 + 4n_{y_{ik}}^4 n_{z_{ik}}^2 + 4n_{y_{ik}}^2 n_{z_{ik}}^4\right).$$

We can deduce that 0 *is a third order eigenvalue of* $\mathbb{B}_{ik}$*, but the three other eigenvalues are not easily specified. Then, we shall use the Sylvester's criteria. For that, we denote by* $\mathbb{B}_{ik} = (b_{jl})_{1\leq j,l\leq 6}$ *the coefficients of the matrix* $\mathbb{B}_{ik}$ *and* $\mathbb{B}_q = (b_{jl})_{1\leq j,l\leq q}$ *the submatrices of* $\mathbb{B}_{ik}$*, and we observe that*

$$\begin{aligned}
det(\mathbb{B}_1) &= \frac{1}{\rho_i v_{p_i}} > 0,\\
det(\mathbb{B}_2) &= \frac{1}{\rho_i^2 v_{p_i} v_{s_i}}\left[4n_{x_{ik}}^2 n_{z_{ik}}^2 + n_{y_{ik}}^2(n_{x_{ik}}^2 + n_{z_{ik}}^2)\right] \geq 0,\\
det(\mathbb{B}_3) &= \frac{9}{\rho_i^3 v_{p_i} v_{s_i}^2} n_{x_{ik}}^2 n_{y_{ik}}^2 n_{z_{ik}}^2 \geq 0,\\
det(\mathbb{B}_4) &= det(\mathbb{B}_5) = det(\mathbb{B}_6) = 0,
\end{aligned}$$

so that the three other eigenvalues of $\mathbb{B}_{ik}$ *are necessarily positive.*

3.4 Time-discretization

At last, we apply a leap-frog time-integration scheme. It is a two steps explicit scheme which results, when combined to the centered fluxes defined at (15), in a non-diffusive scheme (see section 4.2). We note by Δt the time-step and the superscripts refer to time stations. Thus, on each element $\mathcal{T}_i$, $\vec{V}_i^n$ represents the velocity field at $t^n = n\Delta t$ and $\vec{\tilde{\sigma}}_i^{n+\frac{1}{2}}$ the stress tensor components at $t^{n+\frac{1}{2}} = (n+\frac{1}{2})\Delta t$. Starting from initial values $\vec{V}_i^0$ at $t = 0$ and $\vec{\tilde{\sigma}}_i^{\frac{1}{2}}$ at $t = \frac{\Delta t}{2}$, the final scheme expresses on each element $\mathcal{T}_i$ by:

$$\begin{aligned}
\rho_i \int_{\mathcal{T}_i} \vec{\varphi}_i^t \frac{\vec{V}_i^{n+1} - \vec{V}_i^n}{\Delta t}\, dv &= -\sum_{\alpha\in\{x,y,z\}} \int_{\mathcal{T}_i} (\partial_\alpha \vec{\varphi}_i)^t \mathbb{M}_\alpha \vec{\tilde{\sigma}}_i^{n+\frac{1}{2}}\, dv\\
&\quad + \sum_{k\in\mathcal{V}(i)} \int_{S_{ik}} \vec{\varphi}_i^t \mathbb{P}_{ik} \frac{\vec{\tilde{\sigma}}_i^{n+\frac{1}{2}} + \vec{\tilde{\sigma}}_k^{n+\frac{1}{2}}}{2}\, ds\\
&\quad + \sum_{k\in\mathcal{E}(i)} \int_{S_{ik}} \vec{\varphi}_i^t \left[\frac{1}{2}\mathbb{P}_{ik}\ \vec{\tilde{\sigma}}_i^{n+\frac{1}{2}} - \frac{1}{2}\mathbb{A}_{ik}\ \vec{V}_i^n\right] ds\,, \qquad (26)\\
\int_{\mathcal{T}_i} \vec{\psi}_i^t \Lambda_i \frac{\vec{\tilde{\sigma}}_i^{n+\frac{3}{2}} - \vec{\tilde{\sigma}}_i^{n+\frac{1}{2}}}{\Delta t}\, dv &= -\sum_{\alpha\in\{x,y,z\}} \int_{\mathcal{T}_i} (\partial_\alpha \vec{\psi}_i)^t \mathbb{M}_\alpha^t \vec{V}_i^{n+1} dv\\
&\quad + \sum_{k\in\mathcal{V}(i)} \int_{S_{ik}} \vec{\psi}_i^t \mathbb{P}_{ik}^t \frac{\vec{V}_i^{n+1} + \vec{V}_k^{n+1}}{2} ds\\
&\quad + \sum_{k\in\mathcal{E}(i)} \int_{S_{ik}} \vec{\psi}_i^t \left[\frac{1}{2}\mathbb{P}_{ik}^t\ \vec{V}_i^{n+1} - \frac{1}{2}\mathbb{B}_{ik}\ \vec{\tilde{\sigma}}_i^{n+\frac{1}{2}}\right] ds\\
&\quad + \sum_{k\in\mathcal{K}(i)} \int_{S_{ik}} \vec{\psi}_i^t \mathbb{P}_{ik}^t\ \vec{V}_i^{n+1}\, ds\,. \qquad (27)
\end{aligned}$$

Obviously, linear combinations (12) and (13) are still valid with superscripts.

4 Energy preservation and stability of the scheme

The discrete scheme (26)-(27) being explicit, it is conditionally stable. The aim of this section is to establish a sufficient condition on the time step Δt for the L^2-stability of the Discontinuous Galerkin scheme, taking into account both free surface (16) and absorbing boundary conditions (24)-(25). Following [13, 7, 8], we shall define a discrete energy and prove that it is a quadratic positive definite form playing the role of a Lyapunov function of all the unknowns $\vec{V}_i^n$ and $\vec{\tilde{\sigma}}_i^{n-1/2}$.

4.1 A discrete elastodynamic energy

In the continuum, the total energy of the system is given by:

$$E(t) = \underbrace{\frac{1}{2}\int_\Omega \rho \, \|\vec{V}(t)\|^2 \, dv}_{E_k,\, \text{kinetic energy}} + \underbrace{\frac{1}{2}\int_\Omega \overline{\overline{\sigma}}(t) : \overline{\overline{\epsilon}}(t)\, dv}_{E_m,\, \text{mechanical energy}} \quad ,$$

where $\overline{\overline{\epsilon}}$ is the symmetrical deformation tensor whose components are $\epsilon_{i,j} = \frac{1}{2}\left(\frac{\partial U_i}{\partial x_j} + \frac{\partial U_j}{\partial x_i}\right)$. As for the stress, we introduce the deformation vector $\vec{\epsilon} = (\epsilon_{xx}, \epsilon_{yy}, \epsilon_{zz}, 2\,\epsilon_{xy}, 2\,\epsilon_{xz}, 2\,\epsilon_{yz})^t$. For an elastic medium, the generalized Hooke's law links deformations and stresses through the linear relationship $\vec{\epsilon} = C\,\vec{\sigma}$, where the matrix C expresses

$$C = \frac{1}{E}\begin{pmatrix} 1 & -\nu & -\nu & 0 & 0 & 0 \\ -\nu & 1 & -\nu & 0 & 0 & 0 \\ -\nu & -\nu & 1 & 0 & 0 & 0 \\ 0 & 0 & 0 & 2\,(1+\nu) & 0 & 0 \\ 0 & 0 & 0 & 0 & 2\,(1+\nu) & 0 \\ 0 & 0 & 0 & 0 & 0 & 2\,(1+\nu) \end{pmatrix},$$

E and ν being respectively the Young's modulus and the Poisson's ratio

$$E = \frac{\mu\,(3\lambda + 2\mu)}{\lambda + \mu} \quad \text{and} \quad \nu = \frac{\lambda}{2\,(\lambda+\mu)}\,.$$

Thanks to this relationship, the mechanical energy becomes

$$E_m = \frac{1}{2}\int_\Omega (\vec{\sigma})^t\, \vec{\epsilon}\, dv = \frac{1}{2}\int_\Omega (\vec{\sigma})^t\, C\, \vec{\sigma}\, dv\,,$$

and introducing the change of variables (4), we obtain

$$E_m = \frac{1}{2}\int_\Omega \left(\mathbb{T}^{-1}\vec{\tilde{\sigma}}\right)^t C \left(\mathbb{T}^{-1}\vec{\tilde{\sigma}}\right) dv = \frac{1}{2}\int_\Omega \left(\vec{\tilde{\sigma}}\right)^t \left[\left(\mathbb{T}^{-1}\right)^t C\, \mathbb{T}^{-1}\right] \vec{\tilde{\sigma}}\, dv\,.$$

We can easily check that $\left(\mathbb{T}^{-1}\right)^t C\, \mathbb{T}^{-1} = \Lambda$ so that, the total energy writes

$$E(t) = \frac{1}{2}\int_\Omega \rho \|\vec{V}(t)\|^2\, dv + \frac{1}{2}\int_\Omega \left(\vec{\tilde{\sigma}}(t)\right)^t \Lambda(\lambda,\mu)\, \vec{\tilde{\sigma}}(t)\, dv\,.$$

Definition 1 *The discrete energy E^n in three dimensions of space at time $n\Delta t$ is defined by:*

$$E^n \;=\; \frac{1}{2}\sum_{i=1}^{N_T} \int_{\mathcal{T}_i} \left[\rho_i \left(\vec{V}_i^{\,n}\right)^t \vec{V}_i^{\,n} + \left(\vec{\tilde{\sigma}}_i^{\,n+\frac{1}{2}}\right)^t \Lambda_i\, \vec{\tilde{\sigma}}_i^{\,n-\frac{1}{2}}\right] dv\,. \tag{28}$$

4.2 Energy preservation

Now, we study the evolution of the discrete elastodynamic energy through one time-step. More precisely, we aim to establish that the combination between the centered approximation of the fluxes and the leap-frog time-integration leads to a non-dissipative scheme for unbounded domains or domains with free surfaces.

For the simplex $\mathcal{T}_i$, we denote by $\vec{V}_i^{[n+\frac{1}{2}]} = \dfrac{\vec{V}_i^{n+1} + \vec{V}_i^{n}}{2}$ and $\vec{\tilde{\sigma}}_i^{[n]} = \dfrac{\vec{\tilde{\sigma}}_i^{n+\frac{1}{2}} + \vec{\tilde{\sigma}}_i^{n-\frac{1}{2}}}{2}$ the mean-values of the velocity and the stress vectors at times $\left(n+\frac{1}{2}\right)\Delta t$ and $n\Delta t$ respectively.

Lemma 1 *The variation of the total discrete energy during one time-step Δt is*

$$E^{n+1} - E^n \;=\; -\frac{\Delta t}{2}\sum_{i=1}^{N_T}\sum_{k\in\mathcal{E}(i)} \int_{S_{ik}} \left[\left(\vec{V}_i^{[n+\frac{1}{2}]}\right)^t \mathbb{A}_{ik}\, \vec{V}_i^{\,n} + \left(\vec{\tilde{\sigma}}_i^{\,n+\frac{1}{2}}\right)^t \mathbb{B}_{ik}\, \vec{\tilde{\sigma}}_i^{[n]}\right] ds\,. \tag{29}$$

Proof 1 *We calculate the variation of the discrete energy during one time-step Δt:*

$$E^{n+1}-E^n=\sum_{i=1}^{N_T}\int_{\mathcal{T}_i}\left[\rho_i\frac{\left(\vec{V}_i^{n+1}+\vec{V}_i^{n}\right)^t}{2}\left(\vec{V}_i^{n+1}-\vec{V}_i^{n}\right)+\frac{\left(\vec{\tilde{\sigma}}_i^{n+\frac{1}{2}}\right)^t}{2}\Lambda_i\left(\vec{\tilde{\sigma}}_i^{n+\frac{3}{2}}-\vec{\tilde{\sigma}}_i^{n-\frac{1}{2}}\right)\right]dv\,. \tag{30}$$

Thus, we substitute $\vec{\varphi}_i$ and $\vec{\psi}_i$ in (26)-(27) by $\vec{V}_i^{\left[n+\frac{1}{2}\right]}$ and $\vec{\tilde{\sigma}}_i^{n+\frac{1}{2}}$ whose each component belongs to $\mathcal{P}_m(\mathcal{T}_i)$:

$$\begin{aligned}
E^{n+1}-E^n &= -\Delta t\sum_{i=1}^{N_T}\sum_{\alpha\in\{x,y,z\}}\int_{\mathcal{T}_i}\left[\left(\partial_\alpha\vec{V}_i^{\left[n+\frac{1}{2}\right]}\right)^t\mathbb{M}_\alpha\vec{\tilde{\sigma}}_i^{n+\frac{1}{2}}+\left(\partial_\alpha\vec{\tilde{\sigma}}_i^{n+\frac{1}{2}}\right)^t\mathbb{M}_\alpha^t\vec{V}_i^{\left[n+\frac{1}{2}\right]}\right]dv\\
&+\frac{\Delta t}{2}\sum_{i=1}^{N_T}\sum_{k\in\mathcal{V}(i)}\int_{S_{ik}}\left[\left(\vec{V}_i^{\left[n+\frac{1}{2}\right]}\right)^t\mathbb{P}_{ik}\;\vec{\tilde{\sigma}}_k^{n+\frac{1}{2}}+\left(\vec{\tilde{\sigma}}_i^{n+\frac{1}{2}}\right)^t\mathbb{P}_{ik}^t\;\vec{V}_k^{\left[n+\frac{1}{2}\right]}\right]ds\\
&-\frac{\Delta t}{2}\sum_{i=1}^{N_T}\sum_{k\in\mathcal{E}(i)}\int_{S_{ik}}\left[\left(\vec{V}_i^{\left[n+\frac{1}{2}\right]}\right)^t\mathbb{A}_{ik}\;\vec{V}_i^{n}+\left(\vec{\tilde{\sigma}}_i^{n+\frac{1}{2}}\right)^t\mathbb{B}_{ik}\;\vec{\tilde{\sigma}}_i^{[n]}\right]ds\\
&+\frac{\Delta t}{2}\sum_{i=1}^{N_T}\left[\sum_{k\in\mathcal{V}(i)}\int_{S_{ik}}\left[\left(\vec{V}_i^{\left[n+\frac{1}{2}\right]}\right)^t\mathbb{P}_{ik}\;\vec{\tilde{\sigma}}_i^{n+\frac{1}{2}}+\left(\vec{\tilde{\sigma}}_i^{n+\frac{1}{2}}\right)^t\mathbb{P}_{ik}^t\;\vec{V}_i^{\left[n+\frac{1}{2}\right]}\right]ds\right.\\
&\qquad+\sum_{k\in\mathcal{E}(i)}\int_{S_{ik}}\left[\left(\vec{V}_i^{\left[n+\frac{1}{2}\right]}\right)^t\mathbb{P}_{ik}\;\vec{\tilde{\sigma}}_i^{n+\frac{1}{2}}+\left(\vec{\tilde{\sigma}}_i^{n+\frac{1}{2}}\right)^t\mathbb{P}_{ik}^t\;\vec{V}_i^{\left[n+\frac{1}{2}\right]}\right]ds\\
&\qquad\left.+2\sum_{k\in\mathcal{K}(i)}\int_{S_{ik}}\left(\vec{\tilde{\sigma}}_i^{n+\frac{1}{2}}\right)^t\mathbb{P}_{ik}^t\;\vec{V}_i^{\left[n+\frac{1}{2}\right]}\;ds\right].
\end{aligned} \tag{31}$$

By the Green formula, we obtain:

$$\int_{\mathcal{T}_i}\left[\left(\partial_\alpha\vec{V}_i^{\left[n+\frac{1}{2}\right]}\right)^t\mathbb{M}_\alpha\vec{\tilde{\sigma}}_i^{n+\frac{1}{2}}+\left(\partial_\alpha\vec{\tilde{\sigma}}_i^{n+\frac{1}{2}}\right)^t\mathbb{M}_\alpha^t\vec{V}_i^{\left[n+\frac{1}{2}\right]}\right]dv=\int_{\partial\mathcal{T}_i}\left(\vec{V}_i^{\left[n+\frac{1}{2}\right]}\right)^t\mathbb{M}_\alpha\vec{\tilde{\sigma}}_i^{n+\frac{1}{2}}n_{\alpha_i}\,ds\,. \tag{32}$$

Moreover, we clearly have $\left(\vec{\tilde{\sigma}}_i^{n+\frac{1}{2}}\right)^t\mathbb{P}_{ik}^t\;\vec{V}_i^{\left[n+\frac{1}{2}\right]}=\left(\vec{V}_i^{\left[n+\frac{1}{2}\right]}\right)^t\mathbb{P}_{ik}\;\vec{\tilde{\sigma}}_i^{n+\frac{1}{2}}$. Consequently, we deduce that the first and the fourth terms of $E^{n+1}-E^n$ vanish. Further, thanks to the orientation of $n_{\alpha_{ik}}$ from $\mathcal{T}_i$ to $\mathcal{T}_k$, we remark that:

$$\sum_{i=1}^{N_T}\sum_{k\in\mathcal{V}(i)}\int_{S_{ik}}\left(\vec{\tilde{\sigma}}_i^{n+\frac{1}{2}}\right)^t\mathbb{P}_{ik}^t\;\vec{V}_k^{\left[n+\frac{1}{2}\right]}\;ds=-\sum_{i=1}^{N_T}\sum_{k\in\mathcal{V}(i)}\int_{S_{ik}}\left(\vec{V}_i^{\left[n+\frac{1}{2}\right]}\right)^t\mathbb{P}_{ik}\;\vec{\tilde{\sigma}}_k^{n+\frac{1}{2}}\;ds\,,$$

which implies that the second term is also equal to zero. Therefore, it remains only the third term which concludes this proof.

Corollary 1 *Using the scheme (26)-(27), for an infinite domain or a domain including free surface boundaries (16) only, the discrete elastodynamic energy is preserved through one time-step:*

$$\forall n\in\mathbb{N},\quad E^{n+1}=E^n\,.$$

Proof 2 *In an infinite domain or a domain with free surface boundary conditions, $\mathcal{E}(i)$ is an empty set. Therefore, following (29), the discrete elastodynamic energy is preserved.*

4.3 A corrected discrete elastodynamic energy for absorbing boundaries

When absorbing boundary conditions are applied at some faces of the domain (i.e. when $\mathcal{E}(i)$ is not empty), the discrete variation of the energy through one time-step Δt is not necessarily negative according to Lemma 1, because of the time-asymmetry on both $\vec{V}_i$ and $\vec{\tilde{\sigma}}_i$ in (29). In order to overcome this difficulty, we introduce correction terms in the definition of the discrete energy (28) and prove that this corrected discrete elastodynamic energy is not increased through each time step.

Definition 2 *We introduce a corrected discrete elastodynamic energy $\mathcal{E}^n$ at time $n\Delta t$ by:*

$$\mathcal{E}^n = E^n - \frac{\Delta t}{8} \sum_{i=1}^{N_T} \sum_{k\in\mathcal{E}(i)} \int_{S_{ik}} \left[\left(\vec{V}_i^n\right)^t \mathbb{A}_{ik}\ \vec{V}_i^n - \left(\vec{\tilde{\sigma}}_i^{n-\frac{1}{2}}\right)^t \mathbb{B}_{ik}\ \vec{\tilde{\sigma}}_i^{n-\frac{1}{2}} \right] ds. \tag{33}$$

These correction terms only concern the absorbing faces and have no particular physical meaning. However, they match the loss of energy (which appears as a decreasing discrete energy) through these faces since we only consider outgoing waves.

Lemma 2 *The sequel $(\mathcal{E}^n)_{n\in\mathbb{N}}$ is not increasing. More precisely, we have for all $n \in \mathbb{N}$:*

$$\mathcal{E}^{n+1} - \mathcal{E}^n = -\frac{\Delta t}{2} \sum_{i=1}^{N_T} \sum_{k\in\mathcal{E}(i)} \int_{S_{ik}} \left[\left(\vec{V}_i^{[n+\frac{1}{2}]}\right)^t \mathbb{A}_{ik}\ \vec{V}_i^{[n+\frac{1}{2}]} + \left(\vec{\tilde{\sigma}}_i^{[n]}\right)^t \mathbb{B}_{ik}\ \vec{\tilde{\sigma}}_i^{[n]} \right] ds. \tag{34}$$

Proof 3 *We calculate the variation of the total corrected discrete elastodynamic energy:*

$$\begin{aligned}
\mathcal{E}^{n+1} - \mathcal{E}^n \;=\; & -\frac{\Delta t}{4} \sum_{i=1}^{N_T} \sum_{k\in\mathcal{E}(i)} \int_{S_{ik}} \left[\left(\vec{V}_i^n + \vec{V}_i^{n+1}\right)^t \mathbb{A}_{ik}\ \vec{V}_i^n + \left(\vec{\tilde{\sigma}}_i^{n+\frac{1}{2}}\right)^t \mathbb{B}_{ik}\ \left(\vec{\tilde{\sigma}}_i^{n-\frac{1}{2}} + \vec{\tilde{\sigma}}_i^{n+\frac{1}{2}}\right) \right] ds \\
& -\frac{\Delta t}{8} \sum_{i=1}^{N_T} \sum_{k\in\mathcal{E}(i)} \int_{S_{ik}} \left[\left(\vec{V}_i^{n+1}\right)^t \mathbb{A}_{ik}\ \vec{V}_i^{n+1} - \left(\vec{V}_i^n\right)^t \mathbb{A}_{ik}\ \vec{V}_i^n \right] ds \\
& +\frac{\Delta t}{8} \sum_{i=1}^{N_T} \sum_{k\in\mathcal{E}(i)} \int_{S_{ik}} \left[\left(\vec{\tilde{\sigma}}_i^{n+\frac{1}{2}}\right)^t \mathbb{B}_{ik}\ \vec{\tilde{\sigma}}_i^{n+\frac{1}{2}} - \left(\vec{\tilde{\sigma}}_i^{n-\frac{1}{2}}\right)^t \mathbb{B}_{ik}\ \vec{\tilde{\sigma}}_i^{n-\frac{1}{2}} \right] ds\,.
\end{aligned}$$

After a reorganization of the terms by using the symmetry of the matrices $\mathbb{A}_{ik}$ and $\mathbb{B}_{ik}$, the last expression simplifies into (34), which is negative because $\mathbb{A}_{ik}$ and $\mathbb{B}_{ik}$ are respectively a positive definite symmetrical and a semi-positive definite symmetrical matrices.

4.4 Stability of the scheme

We aim at proving that the discrete corrected elastodynamic energy $\mathcal{E}^n$ is a positive definite quadratic form of the unknowns $\vec{V}_i^n$ and $\vec{\tilde{\sigma}}_i^{n-1/2}$ under some stability condition on the time step Δt. For that, we need to introduce another formulation of $\mathcal{E}^n$, independently of the unknowns $\vec{\tilde{\sigma}}_i^{n+1/2}$.

Lemma 3 *The discrete corrected energy $\mathcal{E}^n$, defined at (33), can be rewritten as*

$$\begin{aligned}
\mathcal{E}^n \;=\; & \frac{1}{2} \sum_{i=1}^{N_T} \int_{\mathcal{T}_i} \left[\rho_i \left(\vec{V}_i^n\right)^t \vec{V}_i^n + \left(\vec{\tilde{\sigma}}_i^{n-\frac{1}{2}}\right)^t \Lambda_i \vec{\tilde{\sigma}}_i^{n-\frac{1}{2}} \right] dv \\
+ \; & \frac{\Delta t}{4} \sum_{i=1}^{N_T} \sum_{\alpha\in\{x,y,z\}} \int_{\mathcal{T}_i} \left[\left(\partial_\alpha \vec{V}_i^n\right)^t \mathbb{M}_\alpha \vec{\tilde{\sigma}}_i^{n-\frac{1}{2}} - \left(\partial_\alpha \vec{\tilde{\sigma}}_i^{n-\frac{1}{2}}\right)^t \mathbb{M}_\alpha^t \vec{V}_i^n \right] dv \\
+ \; & \frac{\Delta t}{4} \sum_{i=1}^{N_T} \sum_{k\in\mathcal{V}(i)} \int_{S_{ik}} \left(\vec{\tilde{\sigma}}_i^{n-\frac{1}{2}}\right)^t \mathbb{P}_{ik}^t \vec{V}_k^n ds + \frac{\Delta t}{4} \sum_{i=1}^{N_T} \sum_{k\in\mathcal{K}(i)} \int_{S_{ik}} \left(\vec{\tilde{\sigma}}_i^{n-\frac{1}{2}}\right)^t \mathbb{P}_{ik}^t \vec{V}_i^n ds \\
- \; & \frac{\Delta t}{8} \sum_{i=1}^{N_T} \sum_{k\in\mathcal{E}(i)} \int_{S_{ik}} \left[\left(\vec{V}_i^n\right)^t \mathbb{A}_{ik} \vec{V}_i^n + \left(\vec{\tilde{\sigma}}_i^{n-\frac{1}{2}}\right)^t \mathbb{B}_{ik} \vec{\tilde{\sigma}}_i^{n-\frac{1}{2}} \right] ds.
\end{aligned} \tag{35}$$

Proof 4 *At first, we consider Eq. (27) at the previous time step (as the velocity is at time $n\Delta t$) and we replace $\vec{\psi}_i$ by $\vec{\tilde{\sigma}}_i^{n-\frac{1}{2}}$:*

$$\begin{aligned}\int_{\mathcal{T}_i}\left(\vec{\tilde{\sigma}}_i^{n-\frac{1}{2}}\right)^t\Lambda_i\vec{\tilde{\sigma}}_i^{n+\frac{1}{2}}\,dv &= \int_{\mathcal{T}_i}\left(\vec{\tilde{\sigma}}_i^{n-\frac{1}{2}}\right)^t\Lambda_i\vec{\tilde{\sigma}}_i^{n-\frac{1}{2}}\,dv-\Delta t\sum_{\alpha\in\{x,y,z\}}\int_{\mathcal{T}_i}\left(\partial_\alpha\vec{\tilde{\sigma}}_i^{n-\frac{1}{2}}\right)^t\mathbb{M}_\alpha^t\vec{V}_i^n dv\\ &+\Delta t\sum_{k\in\mathcal{V}(i)}\int_{S_{ik}}\left(\vec{\tilde{\sigma}}_i^{n-\frac{1}{2}}\right)^t\mathbb{P}_{ik}^t\frac{\vec{V}_i^n+\vec{V}_k^n}{2}ds\\ &+\Delta t\sum_{k\in\mathcal{E}(i)}\int_{S_{ik}}\left(\vec{\tilde{\sigma}}_i^{n-\frac{1}{2}}\right)^t\left[\frac{1}{2}\mathbb{P}_{ik}^t\,\vec{V}_i^n-\frac{1}{2}\mathbb{B}_{ik}\,\vec{\tilde{\sigma}}_i^{n-\frac{1}{2}}\right]ds\\ &+\Delta t\sum_{k\in\mathcal{K}(i)}\int_{S_{ik}}\left(\vec{\tilde{\sigma}}_i^{n-\frac{1}{2}}\right)^t\mathbb{P}_{ik}^t\,\vec{V}_i^n\,ds.\end{aligned}$$

Then, we substitute the previous expansion in the definition of the discrete corrected energy (33) and we get:

$$\begin{aligned}\mathcal{E}^n &= \frac{1}{2}\sum_{i=1}^{N_T}\int_{\mathcal{T}_i}\left[\rho_i\left(\vec{V}_i^n\right)^t\vec{V}_i^n+\left(\vec{\tilde{\sigma}}_i^{n-\frac{1}{2}}\right)^t\Lambda_i\vec{\tilde{\sigma}}_i^{n-\frac{1}{2}}-\Delta t\sum_{\alpha\in\{x,y,z\}}\left(\partial_\alpha\vec{\tilde{\sigma}}_i^{n-\frac{1}{2}}\right)^t\mathbb{M}_\alpha^t\vec{V}_i^n\right]dv\\ &+ \frac{\Delta t}{4}\sum_{i=1}^{N_T}\sum_{k\in\mathcal{E}(i)}\int_{S_{ik}}\left[\left(\vec{\tilde{\sigma}}_i^{n-\frac{1}{2}}\right)^t\mathbb{P}_{ik}^t\vec{V}_i^n-\frac{1}{2}\left(\vec{V}_i^n\right)^t\mathbb{A}_{ik}\vec{V}_i^n-\frac{1}{2}\left(\vec{\tilde{\sigma}}_i^{n-\frac{1}{2}}\right)^t\mathbb{B}_{ik}\vec{\tilde{\sigma}}_i^{n-\frac{1}{2}}\right]ds\\ &+ \frac{\Delta t}{4}\sum_{i=1}^{N_T}\sum_{k\in\mathcal{V}(i)}\int_{S_{ik}}\left(\vec{\tilde{\sigma}}_i^{n-\frac{1}{2}}\right)^t\mathbb{P}_{ik}^t\left(\vec{V}_i^n+\vec{V}_k^n\right)ds+\frac{\Delta t}{2}\sum_{i=1}^{N_T}\sum_{k\in\mathcal{K}(i)}\int_{S_{ik}}\left(\vec{\tilde{\sigma}}_i^{n-\frac{1}{2}}\right)^t\mathbb{P}_{ik}^t\vec{V}_i^n ds.\end{aligned}$$

At last, we conclude this proof by applying the Green formula:

$$\begin{aligned}&\sum_{k\in\mathcal{V}(i)}\int_{S_{ik}}\left(\vec{\tilde{\sigma}}_i^{n-\frac{1}{2}}\right)^t\mathbb{P}_{ik}^t\,\vec{V}_i^n\,ds+\sum_{k\in\mathcal{E}(i)}\int_{S_{ik}}\left(\vec{\tilde{\sigma}}_i^{n-\frac{1}{2}}\right)^t\mathbb{P}_{ik}^t\,\vec{V}_i^n\,ds+\sum_{k\in\mathcal{K}(i)}\int_{S_{ik}}\left(\vec{\tilde{\sigma}}_i^{n-\frac{1}{2}}\right)^t\mathbb{P}_{ik}^t\,\vec{V}_i^n\,ds\\ =\;&\sum_{\alpha\in\{x,y,z\}}\int_{\mathcal{T}_i}\left[\left(\partial_\alpha\vec{\tilde{\sigma}}_i^{n-\frac{1}{2}}\right)^t\mathbb{M}_\alpha^t\vec{V}_i^n+\left(\partial_\alpha\vec{V}_i^n\right)^t\mathbb{M}_\alpha\vec{\tilde{\sigma}}_i^{n-\frac{1}{2}}\right]dv.\end{aligned}$$

In what follows, we denote by $S_i=\sum_{k\in\mathcal{V}(i)}S_{ik}+\sum_{k\in\mathcal{K}(i)}S_{ik}+\sum_{k\in\mathcal{E}(i)}S_{ik}\neq 0$ the area of a tetrahedron $\mathcal{T}_i$. Furthermore, we assume that inside each finite element $\mathcal{T}_i$, there exist two positive dimensionless constants $a_i>0$ and $b_{ik}>0$ (for $k\in\mathcal{V}(i)$, $k\in\mathcal{K}(i)$, $k\in\mathcal{E}(i)$) such that, for all polynomial function ϕ defined on $\mathcal{T}_i$:

$$\|\partial_\alpha\phi\|_{\mathrm{L}^2(\mathcal{T}_i)} \leq \frac{a_iS_i}{|\mathcal{T}_i|}\|\phi\|_{\mathrm{L}^2(\mathcal{T}_i)}, \tag{36}$$

$$\|\phi\|^2_{\mathrm{L}^2(S_{ik})} \leq \frac{b_{ik}S_{ik}}{|\mathcal{T}_i|}\|\phi\|^2_{\mathrm{L}^2(\mathcal{T}_i)}, \tag{37}$$

where $\|\phi\|_{\mathrm{L}^2(\mathcal{T}_i)}$ and $\|\phi\|_{\mathrm{L}^2(S_{ik})}$ mean the L^2-norm of ϕ over $\mathcal{T}_i$ and over the face S_{ik} respectively. Note that the constants a_i and b_{ik} do not depend on the size of the finite element $\mathcal{T}_i$ because they are invariant by any homothetic transformation. In fact, they only depend on the geometry of $\mathcal{T}_i$ and on the shapes of ϕ (see [13]). These assumptions will be applied to $\vec{V}_i^n$ and $\vec{\tilde{\sigma}}_i^{n-\frac{1}{2}}$ which are linear combinations of Lagrange polynomial basis functions.

Theorem 1 *Considering the scheme (26)-(27), under assumptions (36) and (37), the corrected total discrete elastodynamic energy $\mathcal{E}^n$ is non-increasing through iterations and is a positive definite quadratic form of all the unknowns $\vec{V}_i^n$ and $\vec{\tilde{\sigma}}_i^{n-1/2}$. Consequently, the scheme is L^2-stable under the CFL type condition:*

$$\begin{aligned}\forall i \in [1, N_T], \qquad & \forall k \in \mathcal{V}(i) \cup \mathcal{K}(i) \cup \mathcal{E}(i) : \\ & \Delta t \left[14a_i + b_{ik} \max(7, r_+(\mathbb{A}_{ik}), r_+(\mathbb{B}_{ik}))\right] < 4\frac{|\mathcal{T}_i|}{S_i} \min\left(\rho_i, r_-\left(\Lambda_i\right)\right),\end{aligned} \tag{38}$$

where we denote by $r_-\left(\Lambda_i\right) = \min\left(\dfrac{1}{2\mu_i}, \dfrac{3}{3\lambda_i + 2\mu_i}\right) > 0$ the smallest eigenvalue of Λ_i, $r_+(\mathbb{A}_{ik}) = \rho_i v_{p_i} > 0$ the greatest eigenvalue of $\mathbb{A}_{ik}$ and $r_+(\mathbb{B}_{ik}) > 0$ the greatest eigenvalue of $\mathbb{B}_{ik}$.

Remark 3 *$\mathbb{B}_{ik}$ is a real symmetrical semi-definite positive matrix by the Sylvester criteria and the eigenvalue 0 has a multiplicity equal to three. Consequently, $\mathbb{B}_{ik}$ has three strictly positive bounded eigenvalues depending only on the material properties (whose expansions are not simple) and then, $r_+(\mathbb{B}_{ik}) > 0$.*

Proof 5 *We can bound down the first term of the right-hand side of (35) in the following way:*

$$\int_{\mathcal{T}_i} \left[\rho_i \left(\vec{V}_i^n\right)^t \vec{V}_i^n + \left(\vec{\tilde{\sigma}}_i^{n-\frac{1}{2}}\right)^t \Lambda_i \vec{\tilde{\sigma}}_i^{n-\frac{1}{2}}\right] dv \geq \rho_i \ \left\|\vec{V}_i^n\right\|^2_{\mathrm{L}^2(\mathcal{T}_i)^3} + r_-(\Lambda_i) \ \left\|\vec{\tilde{\sigma}}_i^{n-\frac{1}{2}}\right\|^2_{\mathrm{L}^2(\mathcal{T}_i)^6}. \tag{39}$$

Then, we set $\|\mathbb{M}\| = \sqrt{r(\mathbb{M}\mathbb{M}^t)}$ where $r(\mathbb{M}\mathbb{M}^t)$ is the spectral radius of the matrix $\mathbb{M}\mathbb{M}^t$. Thus, $\|\mathbb{M}_x\| = \|\mathbb{M}_y\| = 2$ and $\|\mathbb{M}_z\| = 3$, so that $\|\mathbb{P}_{ik}\| \leq \sum_{\alpha\in\{x,y,z\}} \|\mathbb{M}_\alpha\| = 7$. Applying (36), we clearly have:

$$\begin{aligned}\sum_{\alpha\in\{x,y,z\}} \int_{\mathcal{T}_i} \left|\left(\partial_\alpha \vec{V}_i^n\right)^t \mathbb{M}_\alpha \vec{\tilde{\sigma}}_i^{n-\frac{1}{2}} - \left(\partial_\alpha \vec{\tilde{\sigma}}_i^{n-\frac{1}{2}}\right)^t \mathbb{M}_\alpha^t \vec{V}_i^n\right| dv \ &\leq \ 14\frac{a_i S_i}{|\mathcal{T}_i|} \left\|\vec{V}_i^n\right\|_{\mathrm{L}^2(\mathcal{T}_i)^3} \left\|\vec{\tilde{\sigma}}_i^{n-\frac{1}{2}}\right\|_{\mathrm{L}^2(\mathcal{T}_i)^6} \\ &\leq \ 7\frac{a_i S_i}{|\mathcal{T}_i|} \left(\left\|\vec{V}_i^n\right\|^2_{\mathrm{L}^2(\mathcal{T}_i)^3} + \left\|\vec{\tilde{\sigma}}_i^{n-\frac{1}{2}}\right\|^2_{\mathrm{L}^2(\mathcal{T}_i)^6}\right).\end{aligned} \tag{40}$$

On the other hand, using (37) for the internal faces, we also have:

$$\begin{aligned}\int_{S_{ik}} \left|\left(\vec{\tilde{\sigma}}_i^{n-\frac{1}{2}}\right)^t \mathbb{P}_{ik}^t \vec{V}_k^n\right| ds \ &\leq \ \frac{\|\mathbb{P}_{ik}\|}{2} \left(\left\|\vec{V}_k^n\right\|^2_{\mathrm{L}^2(S_{ik})^3} + \left\|\vec{\tilde{\sigma}}_i^{n-\frac{1}{2}}\right\|^2_{\mathrm{L}^2(S_{ik})^6}\right) \\ &\leq \ \frac{7}{2}\left(\frac{b_{ki} S_{ki}}{|\mathcal{T}_k|} \left\|\vec{V}_k^n\right\|^2_{\mathrm{L}^2(\mathcal{T}_k)^3} + \frac{b_{ik} S_{ik}}{|\mathcal{T}_i|} \left\|\vec{\tilde{\sigma}}_i^{n-\frac{1}{2}}\right\|^2_{\mathrm{L}^2(\mathcal{T}_i)^6}\right).\end{aligned} \tag{41}$$

In the very same way, for the boundary faces with free surface condition, we have:

$$\int_{S_{ik}} \left|\left(\vec{\tilde{\sigma}}_i^{n-\frac{1}{2}}\right)^t \mathbb{P}_{ik}^t \vec{V}_i^n\right| ds \leq \frac{7}{2}\frac{b_{ik} S_{ik}}{|\mathcal{T}_i|} \left(\left\|\vec{V}_i^n\right\|^2_{\mathrm{L}^2(\mathcal{T}_i)^3} + \left\|\vec{\tilde{\sigma}}_i^{n-\frac{1}{2}}\right\|^2_{\mathrm{L}^2(\mathcal{T}_i)^6}\right). \tag{42}$$

Then, the last term of the right-hand side of (35) can be bounded thanks to:

$$\begin{aligned}\int_{S_{ik}} \left[\left(\vec{V}_i^n\right)^t \mathbb{A}_{ik} \vec{V}_i^n + \left(\vec{\tilde{\sigma}}_i^{n-\frac{1}{2}}\right)^t \mathbb{B}_{ik} \vec{\tilde{\sigma}}_i^{n-\frac{1}{2}}\right] ds \ &\leq \ r_+(\mathbb{A}_{ik}) \left\|\vec{V}_i^n\right\|^2_{\mathrm{L}^2(S_{ik})^3} + r_+(\mathbb{B}_{ik}) \left\|\vec{\tilde{\sigma}}_i^{n-\frac{1}{2}}\right\|^2_{\mathrm{L}^2(S_{ik})^6} \\ &\leq \ \frac{b_{ik} S_{ik}}{|\mathcal{T}_i|} \left[r_+(\mathbb{A}_{ik}) \left\|\vec{V}_i^n\right\|^2_{\mathrm{L}^2(\mathcal{T}_i)^3} + r_+(\mathbb{B}_{ik}) \left\|\vec{\tilde{\sigma}}_i^{n-\frac{1}{2}}\right\|^2_{\mathrm{L}^2(\mathcal{T}_i)^6}\right].\end{aligned}$$

Therefore, as $S_i = \sum_{k\in\mathcal{V}(i)} S_{ik} + \sum_{k\in\mathcal{K}(i)} S_{ik} + \sum_{k\in\mathcal{E}(i)} S_{ik} \neq 0$ and thanks to the following remark related with (41):

$$\sum_{i=1}^{N_T} \sum_{k\in\mathcal{V}(i)} \frac{b_{ki} S_{ki}}{|\mathcal{T}_k|} \left\|\vec{V}_k^n\right\|^2_{\mathrm{L}^2(\mathcal{T}_k)^3} = \sum_{i=1}^{N_T} \frac{1}{|\mathcal{T}_i|} \left\|\vec{V}_i^n\right\|^2_{\mathrm{L}^2(\mathcal{T}_i)^3} \sum_{k\in\mathcal{V}(i)} b_{ik} S_{ik}, \tag{43}$$

we finally obtain the following estimation:

$$\begin{aligned}
\mathcal{E}^n \;\geq\; & \frac{1}{2}\sum_{i=1}^{N_T}\left\|\vec{V}_i^{\,n}\right\|^2_{\mathrm{L}^2(\mathcal{T}_i)^3}\left[\sum_{k\in\mathcal{V}(i)} S_{ik}\left(\frac{\rho_i}{S_i}-\frac{7}{4}\frac{\Delta t}{|\mathcal{T}_i|}(2a_i+b_{ik})\right)\right.\\
& \qquad +\sum_{k\in\mathcal{K}(i)} S_{ik}\left(\frac{\rho_i}{S_i}-\frac{7}{4}\frac{\Delta t}{|\mathcal{T}_i|}(2a_i+b_{ik})\right)\\
& \qquad \left.+\sum_{k\in\mathcal{E}(i)} S_{ik}\left(\frac{\rho_i}{S_i}-\frac{1}{4}\frac{\Delta t}{|\mathcal{T}_i|}(14a_i+b_{ik}\ r_+(\mathbb{A}_{ik}))\right)\right]\\
& +\frac{1}{2}\sum_{i=1}^{N_T}\left\|\vec{\tilde{\sigma}}_i^{\,n-\frac{1}{2}}\right\|^2_{\mathrm{L}^2(\mathcal{T}_i)^6}\left[\sum_{k\in\mathcal{V}(i)} S_{ik}\left(\frac{r_-(\Lambda_i)}{S_i}-\frac{7}{4}\frac{\Delta t}{|\mathcal{T}_i|}(2a_i+b_{ik})\right)\right.\\
& \qquad +\sum_{k\in\mathcal{K}(i)} S_{ik}\left(\frac{r_-(\Lambda_i)}{S_i}-\frac{7}{4}\frac{\Delta t}{|\mathcal{T}_i|}(2a_i+b_{ik})\right)\\
& \qquad \left.+\sum_{k\in\mathcal{E}(i)} S_{ik}\left(\frac{r_-(\Lambda_i)}{S_i}-\frac{1}{4}\frac{\Delta t}{|\mathcal{T}_i|}(14a_i+b_{ik}\ r_+(\mathbb{B}_{ik}))\right)\right].
\end{aligned}$$

Finally, for any face S_{ik} of the mesh, the discrete corrected energy is a positive definite quadratic form of all the unknowns $\vec{V}_i^{\,n}$ and $\vec{\tilde{\sigma}}_i^{\,n-\frac{1}{2}}$ under the condition (38) on the time step.

Remark 4 *In the condition (38), the ratio $\dfrac{|T_i|}{S_i}$ has the same dimension as the diameter h_i of the finite element $\mathcal{T}_i$, so that (38) is a CFL type stability condition.*

Remark 5 *The condition (38) might be suboptimal. Indeed, when studying this energy in the particular case of the finite volume P_0 approximation, for a uniform mesh with reference tetrahedra (in this case, $a_i = 0$ and $b_{ik} = 1,\ \forall i \in [1, N_T]$), in an infinite domain, we obtain a more precise CFL condition:*

$$v_p\frac{\Delta t}{h} < \frac{\sqrt{2}}{3\sqrt{3}},$$

where $h = \max\limits_{i\in[1,N_T]} h_i$ and the medium is supposed to be homogeneous.
On the other hand, we remark that $\max(7, r_+(\mathbb{A}_{ik}), r_+(\mathbb{B}_{ik})) \geq r_+(\mathbb{A}_{ik}) = \rho v_p$ and $\min(\rho_i, r_-(\Lambda_i)) \leq \rho$, so that in some cases, (38) is simplified by:

$$\forall i \in [1, N_T], \quad v_p\Delta t < 4\frac{|\mathcal{T}_i|}{S_i}, \tag{44}$$

where $|\mathcal{T}_i| = \dfrac{h^3\sqrt{2}}{24}$ and $S_i = \dfrac{h^2(3+\sqrt{3})}{4}$.

Remark 6 *The stability result (38) remains valid when the degree of the polynomial approximation is defined locally and may vary from an element $\mathcal{T}_i$ to its neighbour $\mathcal{T}_k$.*

5 Convergence analysis

The objective of this section is to prove the convergence of the totally discretized scheme (26)-(27) following the method in [13, 28]. We consider a family of unstructured tetrahedral meshes $\mathcal{T}_h$, where $h = \max\limits_{i\in[1,N_T]} h_i$, which forms a partition of the domain Ω, i.e. $\Omega = \cup_{\mathcal{T}_i\in\mathcal{T}_h}\mathcal{T}_i$. We assume that the unstructured meshes $\mathcal{T}_h$ are uniformly *shape regular* in the sense that there exists a constant $\xi > 0$ such that

$$\forall h > 0, \quad \forall \mathcal{T}_i \in \mathcal{T}_h : \qquad \frac{h_i}{d_i} \leq \xi\,, \tag{45}$$

where d_i is the diameter of the biggest ball included in $\mathcal{T}_i$. Moreover, we assume that there exists $\eta > 0$ (independent of h) such that

$$\forall h > 0, \quad \forall \mathcal{T}_i \in \mathcal{T}_h, \quad \forall k \in \mathcal{V}(i) : \qquad \frac{h_k}{h_i} \leq \eta. \tag{46}$$

In what follows, we denote by

$$X_h^1 = \{\vec{\varphi}_h \in \mathrm{L}^2(\Omega)^3 : \quad \forall i,\ \vec{\varphi}_{h_{|\mathcal{T}_i}} \in P_k(\mathcal{T}_i)^3\}, \tag{47}$$

$$X_h^2 = \{\vec{\psi}_h \in \mathrm{L}^2(\Omega)^6 : \quad \forall i,\ \vec{\psi}_{h_{|\mathcal{T}_i}} \in P_k(\mathcal{T}_i)^6\}, \tag{48}$$

the sets of discontinuous piecewise polynomial fields of degree at most k on each $\mathcal{T}_i$. We next introduce the broken Sobolev spaces

$$P\mathrm{H}^s(\Omega) = \left\{v : \quad \forall i,\ v_{|\mathcal{T}_i} \in \mathrm{H}^s(\mathcal{T}_i)\right\} \tag{49}$$

equipped with the norm $\|v\|_{P\mathrm{H}^s(\Omega)} = \left(\sum_{i=1}^{N_T} \|v_{|\mathcal{T}_i}\|^2_{\mathrm{H}^s(\mathcal{T}_i)}\right)^{1/2}$, where $\|\cdot\|_{\mathrm{H}^s(\mathcal{T}_i)}$ denotes the standard H^s-norm on $\mathcal{T}_i$.

5.1 Definition and properties of the semi-discretized scheme

First, we are interested in the study of consistency and stability of the spatially semi-discretized problem below. In what follows, we set $\vec{\varphi}_i$ (resp. $\vec{\psi}_i$) the restriction of $\vec{\varphi} \in \mathrm{H}^s(\mathcal{T}_h)^3$ (resp. $\vec{\psi} \in \mathrm{H}^s(\mathcal{T}_h)^6$) to the element $\mathcal{T}_i$ with $s > \frac{1}{2}$. The semi-discrete solution $(\vec{V}_h, \vec{\tilde{\sigma}}_h)$ defined in $\mathrm{C}^1([0,T], X_h^1 \times X_h^2)$ is the solution of the weak formulation: for any test field $(\vec{\varphi}_h, \vec{\psi}_h) \in X_h^1 \times X_h^2$, for $0 \leq t \leq T$ and all i,

$$\begin{aligned}
\rho_i \int_{\mathcal{T}_i} \vec{\varphi}_i^t \partial_t \vec{V}_i dv &= -\sum_{\alpha\in\{x,y,z\}} \int_{\mathcal{T}_i} (\partial_\alpha \vec{\varphi}_i)^t \mathbb{M}_\alpha \vec{\tilde{\sigma}}_i dv + \sum_{k\in\mathcal{V}(i)} \int_{S_{ik}} \vec{\varphi}_i^t \mathbb{P}_{ik} \frac{\vec{\tilde{\sigma}}_i + \vec{\tilde{\sigma}}_k}{2} ds \\
&\quad + \sum_{k\in\mathcal{E}(i)} \int_{S_{ik}} \vec{\varphi}_i^t \left[\frac{1}{2}\mathbb{P}_{ik}\ \vec{\tilde{\sigma}}_i - \frac{1}{2}\mathbb{A}_{ik}\ \vec{V}_i\right] ds, \qquad (50) \\
\int_{\mathcal{T}_i} \vec{\psi}_i^t \Lambda_i \partial_t \vec{\tilde{\sigma}}_i dv &= -\sum_{\alpha\in\{x,y,z\}} \int_{\mathcal{T}_i} (\partial_\alpha \vec{\psi}_i)^t \mathbb{M}_\alpha^t \vec{V}_i dv + \sum_{k\in\mathcal{V}(i)} \int_{S_{ik}} \vec{\psi}_i^t \mathbb{P}_{ik}^t \frac{\vec{V}_i + \vec{V}_k}{2} ds \\
&\quad + \sum_{k\in\mathcal{E}(i)} \int_{S_{ik}} \vec{\psi}_i^t \left[\frac{1}{2}\mathbb{P}_{ik}^t\ \vec{V}_i - \frac{1}{2}\mathbb{B}_{ik}\ \vec{\tilde{\sigma}}_i\right] ds + \sum_{k\in\mathcal{K}(i)} \int_{S_{ik}} \vec{\psi}_i^t \mathbb{P}_{ik}^t\ \vec{V}_i ds, \qquad (51)
\end{aligned}$$

with the initial values

$$\vec{V}_h(0) = P_h^1(\vec{V}_0) \ \text{ and } \ \vec{\tilde{\sigma}}_h(0) = P_h^2(\vec{\tilde{\sigma}}_0), \tag{52}$$

where $P_h^1 : \mathrm{L}^2(\Omega)^3 \to X_h^1$ and $P_h^2 : \mathrm{L}^2(\Omega)^6 \to X_h^2$ denote respectively the orthogonal projection onto X_h^1 and X_h^2.

Definition 3 *For given vector fields $\vec{W} = (\vec{V}, \vec{\tilde{\sigma}})$ and $\vec{W}' = (\vec{V}', \vec{\tilde{\sigma}}')$, we introduce the following bilinear forms which are well defined on $X_h^1 \times X_h^2$:*

$$m(\vec{W}, \vec{W}') = \sum_{i=1}^{N_T} \int_{\mathcal{T}_i} \left[\rho_i (\vec{V}_i')^t \vec{V}_i + (\vec{\tilde{\sigma}}_i')^t \Lambda_i \vec{\tilde{\sigma}}_i\right] dv \tag{53}$$

$$a(\vec{W}, \vec{W}') = \sum_{i=1}^{N_T} \int_{\mathcal{T}_i} \sum_{\alpha\in\{x,y,z\}} \left[\left(\partial_\alpha \vec{V}_i'\right)^t \mathbb{M}_\alpha \vec{\tilde{\sigma}}_i + \left(\partial_\alpha \vec{\tilde{\sigma}}_i'\right)^t \mathbb{M}_\alpha^t \vec{V}_i\right] dv \tag{54}$$

$$\begin{aligned}
b(\vec{W}, \vec{W}') &= -\sum_{i=1}^{N_T} \sum_{k\in\mathcal{V}(i)} \int_{S_{ik}} \left[(\vec{V}_i')^t \mathbb{P}_{ik} \frac{\vec{\tilde{\sigma}}_i + \vec{\tilde{\sigma}}_k}{2} + (\vec{\tilde{\sigma}}_i')^t \mathbb{P}_{ik}^t \frac{\vec{V}_i + \vec{V}_k}{2}\right] ds \\
&\quad -\frac{1}{2}\sum_{i=1}^{N_T} \sum_{k\in\mathcal{E}(i)} \int_{S_{ik}} \left[(\vec{V}_i')^t \left(\mathbb{P}_{ik}\vec{\tilde{\sigma}}_i - \mathbb{A}_{ik}\vec{V}_i\right) + (\vec{\tilde{\sigma}}_i')^t \left(\mathbb{P}_{ik}^t \vec{V}_i - \mathbb{B}_{ik}\vec{\tilde{\sigma}}_i\right)\right] ds \\
&\quad -\sum_{i=1}^{N_T} \sum_{k\in\mathcal{K}(i)} \int_{S_{ik}} (\vec{\tilde{\sigma}}_i')^t \mathbb{P}_{ik}^t \vec{V}_i\, ds. \qquad (55)
\end{aligned}$$

Thanks to (50) and (51), we remark the following result:

Proposition 1 *The semi-discrete solution $\vec{W}_h = (\vec{V}_h, \vec{\bar{\sigma}}_h)$ of (50)-(51)-(52) satisfies*

$$m(\partial_t \vec{W}_h, \vec{W}'_h) + a(\vec{W}_h, \vec{W}'_h) + b(\vec{W}_h, \vec{W}'_h) = 0, \ \forall \vec{W}'_h \in X_h^1 \times X_h^2. \tag{56}$$

Proposition 2 *The exact solution $\vec{W} = (\vec{V}, \vec{\bar{\sigma}})$ of (6)-(7)-(8)-(9) satisfies the following property*

$$m(\partial_t \vec{W}, \vec{W}'_h) + a(\vec{W}, \vec{W}'_h) + b(\vec{W}, \vec{W}'_h) = 0, \ \forall \vec{W}'_h \in X_h^1 \times X_h^2. \tag{57}$$

Proof 6 *According to (10a)-(10b), we have to verify that the quantity $b(\vec{W}, \vec{W}'_h)$ is equal to*

$$-\sum_{i=1}^{N_T} \sum_{\alpha \in \{x,y,z\}} \int_{\partial \mathcal{T}_i} \left[\left(\vec{V}'_i\right)^t \mathbb{M}_\alpha \vec{\bar{\sigma}} n_{\alpha_i} + \left(\vec{\bar{\sigma}}'_i\right)^t \mathbb{M}_\alpha^t \vec{V} n_{\alpha_i} \right] ds. \tag{58}$$

The free surface boundary condition (7) results in $\displaystyle\sum_{i=1}^{N_T} \sum_{k \in \mathcal{K}(i)} \int_{S_{ik}} (\vec{V}'_i)^t \mathbb{P}_{ik} \vec{\bar{\sigma}} \, ds = 0$. On the other hand, thanks to the absorbing boundary conditions (8), we also have:

$$\begin{aligned} & \frac{1}{2} \sum_{i=1}^{N_T} \sum_{k \in \mathcal{E}(i)} \int_{S_{ik}} \left[(\vec{V}'_i)^t \left(\mathbb{P}_{ik} \vec{\bar{\sigma}} - \mathbb{A}_{ik} \vec{V} \right) + (\vec{\bar{\sigma}}'_i)^t \left(\mathbb{P}_{ik}^t \vec{V} - \mathbb{B}_{ik} \vec{\bar{\sigma}} \right) \right] ds \\ = & \sum_{i=1}^{N_T} \sum_{k \in \mathcal{E}(i)} \int_{S_{ik}} \left[(\vec{V}'_i)^t \mathbb{P}_{ik} \vec{\bar{\sigma}} + (\vec{\bar{\sigma}}'_i)^t \mathbb{P}_{ik}^t \vec{V} \right] ds, \end{aligned} \tag{59}$$

which closes the proof.

Lemma 4 *For any $\vec{W}_h = (\vec{\varphi}_h, \vec{\psi}_h) \in X_h^1 \times X_h^2$, the following quantity is positive:*

$$a(\vec{W}_h, \vec{W}_h) + b(\vec{W}_h, \vec{W}_h) = \frac{1}{2} \sum_{i=1}^{N_T} \sum_{k \in \mathcal{E}(i)} \int_{S_{ik}} \left[\vec{\varphi}_i^t \mathbb{A}_{ik} \vec{\varphi}_i + \vec{\psi}_i^t \mathbb{B}_{ik} \vec{\psi}_i \right] ds \geq 0 \, . \tag{60}$$

Proof 7 *Let be $\vec{W}_h = (\vec{\varphi}_h, \vec{\psi}_h) \in X_h^1 \times X_h^2$ a given vector field. Then, we get*

$$\begin{aligned} a(\vec{W}_h, \vec{W}_h) + b(\vec{W}_h, \vec{W}_h) = & \left[\sum_{i=1}^{N_T} \sum_{\alpha \in \{x,y,z\}} \int_{\mathcal{T}_i} \left[(\partial_\alpha \vec{\varphi}_i)^t \mathbb{M}_\alpha \vec{\psi}_i + \left(\partial_\alpha \vec{\psi}_i\right)^t \mathbb{M}_\alpha^t \vec{\varphi}_i \right] dv \right. \\ & - \frac{1}{2} \sum_{i=1}^{N_T} \sum_{k \in \mathcal{V}(i)} \int_{S_{ik}} \left[\vec{\varphi}_i^t \mathbb{P}_{ik} \vec{\psi}_i + \vec{\psi}_i^t \mathbb{P}_{ik}^t \vec{\varphi}_i \right] ds - \sum_{i=1}^{N_T} \sum_{k \in \mathcal{K}(i)} \int_{S_{ik}} \vec{\psi}_i^t \mathbb{P}_{ik}^t \vec{\varphi}_i ds \\ & \left. - \frac{1}{2} \sum_{i=1}^{N_T} \sum_{k \in \mathcal{E}(i)} \int_{S_{ik}} \left[\vec{\varphi}_i^t \mathbb{P}_{ik} \vec{\psi}_i + \vec{\psi}_i^t \mathbb{P}_{ik}^t \vec{\varphi}_i \right] ds \right] \\ & - \frac{1}{2} \sum_{i=1}^{N_T} \sum_{k \in \mathcal{V}(i)} \int_{S_{ik}} \left[\vec{\varphi}_i^t \mathbb{P}_{ik} \vec{\psi}_k + \vec{\psi}_i^t \mathbb{P}_{ik}^t \vec{\varphi}_k \right] ds \\ & + \frac{1}{2} \sum_{i=1}^{N_T} \sum_{k \in \mathcal{E}(i)} \int_{S_{ik}} \left[\vec{\varphi}_i^t \mathbb{A}_{ik} \vec{\varphi}_i + \vec{\psi}_i^t \mathbb{B}_{ik} \vec{\psi}_i \right] ds \, . \end{aligned}$$

The first term (between brackets) vanishes by the Green Formula:

$$\int_{\mathcal{T}_i} \left[(\partial_\alpha \vec{\varphi}_i)^t \mathbb{M}_\alpha \vec{\psi}_i + \left(\partial_\alpha \vec{\psi}_i\right)^t \mathbb{M}_\alpha^t \vec{\varphi}_i \right] dv = \int_{\partial \mathcal{T}_i} \vec{\varphi}_i^t \mathbb{M}_\alpha n_{\alpha_i} \vec{\psi}_i \, ds, \tag{61}$$

combined to the equality $\vec{\psi}_i^t \mathbb{P}_{ik}^t \vec{\varphi}_i = \vec{\varphi}_i^t \mathbb{P}_{ik} \vec{\psi}_i$. *Moreover, since* $\mathbb{P}_{ik} = \sum_{\alpha \in \{x,y,z\}} \mathbb{M}_\alpha n_{\alpha_{ik}}$ *and thanks to the orientation of* $\vec{\mathbf{n}}_{ik}$ *from* $\mathcal{T}_i$ *to* $\mathcal{T}_k$, *we remark that:*

$$\sum_{i=1}^{N_T} \sum_{k \in \mathcal{V}(i)} \int_{S_{ik}} \vec{\psi}_i^t \mathbb{P}_{ik}^t \vec{\varphi}_k \, ds = - \sum_{i=1}^{N_T} \sum_{k \in \mathcal{V}(i)} \int_{S_{ik}} \vec{\varphi}_i^t \mathbb{P}_{ik} \vec{\psi}_k \, ds \,,$$

which implies that the second term is also equal to zero. Therefore, it remains only the third term depending on $\mathbb{A}_{ik}$ *and* $\mathbb{B}_{ik}$, *which are respectively a real symmetrical definite positive matrix and a real symmetrical semi-definite positive matrix.*

Consequently, if we define the semi-discrete energy by

$$\mathcal{E}_h(t) = \frac{1}{2} m(\vec{W}_h(t), \vec{W}_h(t)), \tag{62}$$

where $\vec{W}_h(t) = (\vec{V}_h(t), \vec{\tilde{\sigma}}_h(t))$ is the semi-discrete solution of (50)-(51)-(52), we deduce from Prop. 1 and Lemma 4 that

$$\partial_t \mathcal{E}_h(t) \leq 0, \forall t \in [0,T], \tag{63}$$

which implies that $\mathcal{E}_h(t)$ is decreasing on $[0,T]$ and we have

$$\mathcal{E}_h(t) \leq \mathcal{E}_h(0) \leq E(0), \quad \forall t \in [0,T]. \tag{64}$$

5.2 Convergence of the semi-discretized problem

We shall at first give a convergence result for the spatially semi-discretized scheme (50)-(51)-(52). We recall the two following lemmae, well-known in the framework of the finite elements (see [10]):

Lemma 5 *Let* $\mathcal{T}_i \in \mathcal{T}_h$, *we assume that* u *belongs to the space* $\mathrm{H}^{s+1}(\mathcal{T}_i)$ *for* $s \geq 0$. *Let* Π *be a linear continuous operator from* $\mathrm{H}^{s+1}(\mathcal{T}_i)$ *onto* $P_k(\mathcal{T}_i)$ *such that* $\Pi(u) = u$ *for all* $u \in P_k(\mathcal{T}_i)$. *Then we have*

$$\|u - \Pi(u)\|_{\mathrm{L}^2(T_i)} \leq C_1 \; h_i^{\min\{s,k\}+1} \; \|u\|_{\mathrm{H}^{s+1}(\mathcal{T}_i)}, \tag{65}$$

$$\|u - \Pi(u)\|_{\mathrm{L}^2(\partial\mathcal{T}_i)} \leq C_1 \; h_i^{\min\{s,k\}+1/2} \; \|u\|_{\mathrm{H}^{s+1}(\mathcal{T}_i)}, \tag{66}$$

where C_1 *is a positive constant only depending on* k, s *and the regularity parameter* ξ *of the mesh.*

Lemma 6 *For all* $p \in P_k(\mathcal{T}_i)$, *we have*

$$\|p\|_{\mathrm{L}^2(\partial\mathcal{T}_i)} \leq C_2 \; h_i^{-1/2} \; \|p\|_{\mathrm{L}^2(\mathcal{T}_i)}, \tag{67}$$

where C_2 *is a positive constant only depending on* k *and the regularity parameter* ξ *of the mesh.*

Thus, we can state the following Lemma:

Lemma 7 *Let be* $\vec{W} = (\vec{V}, \vec{\tilde{\sigma}})$ *the exact solution of (6)-(7)-(8)-(9) supposed to belong to* $\mathrm{C}^0((0,T), P\mathrm{H}^{s+1}(\Omega)^9)$ *and* $(\vec{V}_h, \vec{\tilde{\sigma}}_h) \in \mathrm{C}^1((0,T), X_h^1 \times X_h^2)$ *be the solution of the semi-discrete problem (50)-(51)-(52). For any* $t \in [0,T]$, *we have*

$$\begin{aligned} & b(\vec{W} - P_h^0(\vec{W}), \vec{W}_h - P_h^0(\vec{W}))(t) \\ \leq \; & K h^{\min\{s,k\}} \left[\|(\vec{V}_h - P_h^1(\vec{V}))(t)\|^2_{\mathrm{L}^2(\Omega)^3} + \|(\vec{\tilde{\sigma}}_h - P_h^2(\vec{\tilde{\sigma}}))(t)\|^2_{\mathrm{L}^2(\Omega)^6} \right]^{1/2} \|(\vec{V}, \vec{\tilde{\sigma}})(t)\|_{P\mathrm{H}^{s+1}(\Omega)^9}. \end{aligned} \tag{68}$$

Proof 8 *The two previous Lemmae 5 and 6 imply together the following estimates:*

$$\int_{S_{il}} (\vec{V}_h - P_h^1(\vec{V}))_{|_{\mathcal{T}_i}} \mathbb{P}_{il} (\vec{\tilde{\sigma}} - P_h^2(\vec{\tilde{\sigma}}))_{|_{\mathcal{T}_i}} ds \leq C \; \|\mathbb{P}_{il}\| \; h_i^{\min\{s,k\}} \; \|\vec{V}_h - P_h^1(\vec{V})\|_{\mathrm{L}^2(\mathcal{T}_i)^3} \; \|\vec{\tilde{\sigma}}\|_{\mathrm{H}^{s+1}(\mathcal{T}_i)^6}, \tag{69}$$

$$\int_{S_{il}} (\vec{\tilde{\sigma}}_h - P_h^2(\vec{\tilde{\sigma}}))_{|_{\mathcal{T}_i}} \mathbb{P}_{il}^t (\vec{V} - P_h^1(\vec{V}))_{|_{\mathcal{T}_i}} ds \leq C \; \|\mathbb{P}_{il}\| \; h_i^{\min\{s,k\}} \; \|\vec{\tilde{\sigma}}_h - P_h^2(\vec{\tilde{\sigma}})\|_{\mathrm{L}^2(\mathcal{T}_i)^6} \; \|\vec{V}\|_{\mathrm{H}^{s+1}(\mathcal{T}_i)^3}, \tag{70}$$

$$\int_{S_{il}} (\vec{V}_h - P_h^1(\vec{V}))_{|_{\mathcal{T}_i}} \mathbb{A}_{il} (\vec{V} - P_h^1(\vec{V}))_{|_{\mathcal{T}_i}} ds \leq C \; r_+(\mathbb{A}_{il}) \; h_i^{\min\{s,k\}} \; \|\vec{V}_h - P_h^1(\vec{V})\|_{\mathrm{L}^2(\mathcal{T}_i)^3} \; \|\vec{V}\|_{\mathrm{H}^{s+1}(\mathcal{T}_i)^3}, \tag{71}$$

$$\int_{S_{il}} (\vec{\tilde{\sigma}}_h - P_h^2(\vec{\tilde{\sigma}}))_{|_{\mathcal{T}_i}} \mathbb{B}_{il} (\vec{\tilde{\sigma}} - P_h^2(\vec{\tilde{\sigma}}))_{|_{\mathcal{T}_i}} ds \leq C \; r_+(\mathbb{B}_{il}) \; h_i^{\min\{s,k\}} \; \|\vec{\tilde{\sigma}}_h - P_h^2(\vec{\tilde{\sigma}})\|_{\mathrm{L}^2(\mathcal{T}_i)^6} \; \|\vec{\tilde{\sigma}}\|_{\mathrm{H}^{s+1}(\mathcal{T}_i)^6}, \tag{72}$$

where $C = C_1C_2$, $l \in \mathcal{V}(i) \cup \mathcal{E}(i)$ in (69), $l \in \mathcal{V}(i) \cup \mathcal{K}(i) \cup \mathcal{E}(i)$ in (70), $l \in \mathcal{E}(i)$ in (71)-(72). In addition, applying (46), we have in the same way, for all $l \in \mathcal{V}(i)$:

$$\begin{aligned} & \int_{S_{il}} (\vec{V}_h - P_h^1(\vec{V}))_{|\mathcal{T}_i} \mathbb{P}_{il} (\vec{\tilde{\sigma}} - P_h^2(\vec{\tilde{\sigma}}))_{|\mathcal{T}_l} ds \\ \leq \; & C \, \|\mathbb{P}_{il}\| \, \eta^{\min\{s,k\}+1/2} \, h_i^{\min\{s,k\}} \, \|\vec{V}_h - P_h^1(\vec{V})\|_{\mathrm{L}^2(\mathcal{T}_i)^3} \, \|\vec{\tilde{\sigma}}\|_{\mathrm{H}^{s+1}(\mathcal{T}_l)^6}, \end{aligned} \tag{73}$$

$$\begin{aligned} & \int_{S_{il}} (\vec{\tilde{\sigma}}_h - P_h^2(\vec{\tilde{\sigma}}))_{|\mathcal{T}_i} \mathbb{P}_{il}^t (\vec{V} - P_h^1(\vec{V}))_{|\mathcal{T}_l} ds \\ \leq \; & C \, \|\mathbb{P}_{il}\| \, \eta^{\min\{s,k\}+1/2} \, h_i^{\min\{s,k\}} \, \|\vec{\tilde{\sigma}}_h - P_h^2(\vec{\tilde{\sigma}})\|_{\mathrm{L}^2(\mathcal{T}_i)^6} \, \|\vec{V}\|_{\mathrm{H}^{s+1}(\mathcal{T}_l)^3}. \end{aligned} \tag{74}$$

Theorem 2 *Let $(\mathcal{T}_h)_h$ be a family of unstructured meshes satisfying (45) and (46).*
Let $(\vec{V}, \vec{\tilde{\sigma}})$ be the exact solution of the symmetrical pseudo-conservative problem (6)-(7)-(8)-(9) supposed to belong to $\mathrm{C}^0([0,T]; P\mathrm{H}^{s+1}(\Omega)^9)$ for $s \geq 0$, and let $(\vec{V}_h, \vec{\tilde{\sigma}}_h) \in \mathrm{C}^1([0,T], X_h^1 \times X_h^2)$ be the solution of the semi-discrete problem (50)-(51)-(52). Then, there exists a constant $K > 0$ independent of h such that

$$\max_{t\in[0,T]} \left[\|(\vec{V} - \vec{V}_h)(t)\|^2_{\mathrm{L}^2(\Omega)^3} + \|(\vec{\tilde{\sigma}} - \vec{\tilde{\sigma}}_h)(t)\|^2_{\mathrm{L}^2(\Omega)^6} \right]^{1/2} \leq K T h^{\min\{s,k\}} \|(\vec{V}, \vec{\tilde{\sigma}})\|_{\mathrm{C}^0((0,T), P\mathrm{H}^{s+1}(\Omega)^9)}. \tag{75}$$

Proof 9 *First, applying Lemma 4 to the vector $\vec{W}_h - P_h^0(\vec{W}) = (\vec{V}_h - P_h^1(\vec{V}), \vec{\tilde{\sigma}}_h - P_h^2(\vec{\tilde{\sigma}})) \in X_h^1 \times X_h^2$, we get*

$$a(\vec{W}_h - P_h^0(\vec{W}), \vec{W}_h - P_h^0(\vec{W})) + b(\vec{W}_h - P_h^0(\vec{W}), \vec{W}_h - P_h^0(\vec{W})) \geq 0,$$

and, then

$$\begin{aligned} m(\partial_t(\vec{W}_h - P_h^0(\vec{W})), \vec{W}_h - P_h^0(\vec{W})) \; \leq \; & m(\partial_t(\vec{W}_h - P_h^0(\vec{W})), \vec{W}_h - P_h^0(\vec{W})) \\ + \; & a(\vec{W}_h - P_h^0(\vec{W}), \vec{W}_h - P_h^0(\vec{W})) \\ + \; & b(\vec{W}_h - P_h^0(\vec{W}), \vec{W}_h - P_h^0(\vec{W})). \end{aligned} \tag{76}$$

Thus, since $\vec{W}_h - P_h^0(\vec{W}) \in X_h^1 \times X_h^2$, the difference between (56) and (57) gives us

$$m(\partial_t(\vec{W}_h - \vec{W}), \vec{W}_h - P_h^0(\vec{W})) + a(\vec{W}_h - \vec{W}, \vec{W}_h - P_h^0(\vec{W})) + b(\vec{W}_h - \vec{W}, \vec{W}_h - P_h^0(\vec{W})) = 0.$$

After, we substract the previous equality in the right-hand side of (76) and we obtain

$$\begin{aligned} m(\partial_t(\vec{W}_h - P_h^0(\vec{W})), \vec{W}_h - P_h^0(\vec{W})) \; \leq \; & m(\partial_t(\vec{W} - P_h^0(\vec{W})), \vec{W}_h - P_h^0(\vec{W})) \\ + \; & a(\vec{W} - P_h^0(\vec{W}), \vec{W}_h - P_h^0(\vec{W})) \\ + \; & b(\vec{W} - P_h^0(\vec{W}), \vec{W}_h - P_h^0(\vec{W})). \end{aligned} \tag{77}$$

As $P_h^1(\vec{V})$ (resp. $P_h^2(\vec{\tilde{\sigma}})$) is the orthogonal projection of $\vec{V}$ (resp. $\vec{\tilde{\sigma}}$) onto X_h^1 (resp. X_h^2) and $\vec{W}_h - P_h^0(\vec{W}) \in X_h^1 \times X_h^2$, we necessarily have

$$a(\vec{W} - P_h^0(\vec{W}), \vec{W}_h - P_h^0(\vec{W})) = 0 \tag{78}$$

and

$$m(\partial_t(\vec{W} - P_h^0(\vec{W})), \vec{W}_h - P_h^0(\vec{W})) = \frac{1}{2} \frac{d}{dt} m((\vec{W} - P_h^0(\vec{W})), \vec{W}_h - P_h^0(\vec{W})) = 0. \tag{79}$$

On the other hand, we can check that

$$\begin{aligned} & m(\partial_t(\vec{W}_h - P_h^0(\vec{W})), \vec{W}_h - P_h^0(\vec{W})) \\ = \; & \frac{1}{2} \sum_{i=1}^{N_T} \frac{d}{dt} \int_{T_i} \left[\rho_i \left| \vec{V}_h - P_h^1(\vec{V}) \right|^2 (t) + \left(\left(\vec{\tilde{\sigma}}_h - P_h^2(\vec{\tilde{\sigma}}) \right) \Lambda_i \left(\vec{\tilde{\sigma}}_h - P_h^2(\vec{\tilde{\sigma}}) \right) \right) (t) \right] dv \end{aligned} \tag{80}$$

so, by taking also into account (78) and (79) in (77), we obtain

$$\begin{aligned} & \frac{d}{dt} \left[\|(\vec{V}_h - P_h^1(\vec{V}))(t)\|^2_{\mathrm{L}^2(\Omega)^3} + \|(\vec{\tilde{\sigma}}_h - P_h^2(\vec{\tilde{\sigma}}))(t)\|^2_{\mathrm{L}^2(\Omega)^6} \right] dv \\ \leq \; & 2 \left(\min_{1\leq i\leq N_T} \{\rho_i, r_-(\Lambda_i)\} \right)^{-1} b(\vec{W} - P_h^0(\vec{W}), \vec{W}_h - P_h^0(\vec{W}))(t). \end{aligned} \tag{81}$$

Then, we integrate (81) from 0 *to* $t \in [0,T]$ *and, since (9) and (52) hold, we have*

$$\begin{aligned} & \|(\vec{V}_h - P_h^1(\vec{V}))(t)\|^2_{\mathrm{L}^2(\Omega)^3} + \|(\vec{\tilde{\sigma}}_h - P_h^2(\vec{\tilde{\sigma}}))(t)\|^2_{\mathrm{L}^2(\Omega)^6} \\ \leq \quad & 2\left(\min_{1\leq i\leq N_T}\{\rho_i, r_-(\Lambda_i)\}\right)^{-1} \int_0^T b(\vec{W} - P_h^0(\vec{W}), \vec{W}_h - P_h^0(\vec{W}))(t)dt. \end{aligned} \tag{82}$$

Therefore, the last inequality becomes

$$\max_{t\in[0,T]} \left[\|(\vec{V}_h - P_h^1(\vec{V}))(t)\|^2_{\mathrm{L}^2(\Omega)^3} + \|(\vec{\tilde{\sigma}}_h - P_h^2(\vec{\tilde{\sigma}}))(t)\|^2_{\mathrm{L}^2(\Omega)^6}\right] \tag{83}$$

$$\leq \quad 2\left(\min_{1\leq i\leq N_T}\{\rho_i, r_-(\Lambda_i)\}\right)^{-1} \int_0^T b(\vec{W} - P_h^0(\vec{W}), \vec{W}_h - P_h^0(\vec{W}))(t)dt \tag{84}$$

which implies, by Lemma 7, that there exists $K > 0$ *such that*

$$\max_{t\in[0,T]} \left[\|(\vec{V}_h - P_h^1(\vec{V}))(t)\|^2_{\mathrm{L}^2(\Omega)^3} + \|(\vec{\tilde{\sigma}}_h - P_h^2(\vec{\tilde{\sigma}}))(t)\|^2_{\mathrm{L}^2(\Omega)^6}\right]^{1/2} \leq KTh^{\min\{s,k\}} \|(\vec{V}, \vec{\tilde{\sigma}})\|_{\mathrm{C}^0((0,T),P\mathrm{H}^{s+1}(\Omega)^9)}. \tag{85}$$

On the other hand, we also have by Lemma 5 the existence of $C > 0$ *such that:*

$$\begin{aligned} \forall t \in [0,T], \qquad & \left[\|(\vec{V} - P_h^1(\vec{V}))(t)\|^2_{\mathrm{L}^2(\Omega)^3} + \|(\vec{\tilde{\sigma}} - P_h^2(\vec{\tilde{\sigma}}))(t)\|^2_{\mathrm{L}^2(\Omega)^6}\right]^{1/2} \\ \leq \quad & Ch^{\min\{s,k\}+1}\left(\|\vec{V}(t)\|^2_{P\mathrm{H}^{s+1}(\Omega)^3} + \|\vec{\tilde{\sigma}}(t)\|^2_{P\mathrm{H}^{s+1}(\Omega)^6}\right)^{1/2}, \end{aligned} \tag{86}$$

which combined to (85) concludes the proof.

5.3 Convergence of the totally discretized problem

In this section, we prove the convergence of the totally discretized scheme (26)-(27), following the method proposed in [28].

Theorem 3 *Let* α *be a coefficient such that* $\alpha = 1$ *if absorbing boundary conditions are included in the scheme, or* $\alpha = 2$ *for domains with only free surface boundary conditions. Let* $(\vec{V}, \vec{\tilde{\sigma}})$ *be the exact solution of (6)-(7)-(8)-(9), supposed to belong to* $\mathrm{C}^{2\alpha-1}([0,T], \mathrm{L}^2(\Omega)^9) \cap \mathrm{C}^0([0,T], P\mathrm{H}^{s+1}(\Omega)^9)$*. Let* $(\vec{V}_h^n, \vec{\tilde{\sigma}}_h^{n+1/2})$ *be the solution of (26)-(27). Under a CFL condition of the same type as (38), there exists a constant* $C > 0$ *such that the following error estimate holds:*

$$\begin{aligned} & \max_{n=0,\ldots,N}\left(\|\vec{V}(t_n) - \vec{V}_h^n\|^2_{\mathrm{C}^0([0,T],\mathrm{L}^2(\Omega)^3)} + \|\vec{\tilde{\sigma}}(t_{n+1/2}) - \vec{\tilde{\sigma}}_h^{n+1/2}\|^2_{\mathrm{C}^0([0,T],\mathrm{L}^2(\Omega)^6)}\right)^{1/2} \\ \leq \quad & C\left(\Delta t^\alpha + h^{\min(s,k)}\right)\left(\|(\vec{V}, \vec{\tilde{\sigma}})\|_{\mathrm{C}^{2\alpha-1}([0,T],\mathrm{L}^2(\Omega)^9)} + \|(\vec{V}, \vec{\tilde{\sigma}})\|_{\mathrm{C}^0([0,T],P\mathrm{H}^{s+1}(\Omega)^9)}\right). \end{aligned} \tag{87}$$

Proof 10 *Let* $(\vec{V}_h, \vec{\tilde{\sigma}}_h) \in \mathrm{C}^1([0,T], X_h^1 \times X_h^2)$ *be the solution of the semi-discrete problem (50)-(51)-(52). We are interested in the estimation of the following local consistency error:*

$$\epsilon_h^n = \left(\|\widehat{\vec{V}_h^n} - \vec{V}_h(t_n)\|^2_{\mathrm{L}^2(\Omega)^3} + \|\widehat{\vec{\tilde{\sigma}}_h^{n+\frac{1}{2}}} - \vec{\tilde{\sigma}}_h(t_{n+\frac{1}{2}})\|^2_{\mathrm{L}^2(\Omega)^6}\right)^{1/2}, \tag{88}$$

where $(\vec{\varphi}_h, \vec{\psi}_h) \in X_h^1 \times X_h^2$ *and* $(\widehat{\vec{V}_h^{n+1}}, \widehat{\vec{\bar{\sigma}}_h^{n+1/2}})$ *has been computed as follows:*

$$\begin{aligned}
\rho_i \int_{\mathcal{T}_i} \vec{\varphi}_i^t \frac{\widehat{\vec{V}_i^{n+1}} - \vec{V}_i(t_n)}{\Delta t}\, dv &= -\sum_{\alpha\in\{x,y,z\}} \int_{\mathcal{T}_i} (\partial_\alpha \vec{\varphi}_i)^t \mathbb{M}_\alpha \vec{\bar{\sigma}}_i(t_{n+\frac{1}{2}})\, dv \\
&\quad + \sum_{k\in\mathcal{V}(i)} \int_{S_{ik}} \vec{\varphi}_i^t \mathbb{P}_{ik} \frac{\vec{\bar{\sigma}}_i(t_{n+\frac{1}{2}}) + \vec{\bar{\sigma}}_k(t_{n+\frac{1}{2}})}{2}\, ds \\
&\quad + \sum_{k\in\mathcal{E}(i)} \int_{S_{ik}} \vec{\varphi}_i^t \left[\frac{1}{2}\mathbb{P}_{ik}\ \vec{\bar{\sigma}}_i(t_{n+\frac{1}{2}}) - \frac{1}{2}\mathbb{A}_{ik}\ \vec{V}_i(t_n)\right]\, ds\,, \qquad (89)
\end{aligned}$$

$$\begin{aligned}
\int_{\mathcal{T}_i} \vec{\psi}_i^t \Lambda_i \frac{\widehat{\vec{\bar{\sigma}}_i^{n+\frac{3}{2}}} - \vec{\bar{\sigma}}_i(t_{n+\frac{1}{2}})}{\Delta t}\, dv &= -\sum_{\alpha\in\{x,y,z\}} \int_{\mathcal{T}_i} (\partial_\alpha \vec{\psi}_i)^t \mathbb{M}_\alpha^t \vec{V}_i(t_{n+1}) dv \\
&\quad + \sum_{k\in\mathcal{V}(i)} \int_{S_{ik}} \vec{\psi}_i^t \mathbb{P}_{ik}^t \frac{\vec{V}_i(t_{n+1}) + \vec{V}_k(t_{n+1})}{2} ds \\
&\quad + \sum_{k\in\mathcal{E}(i)} \int_{S_{ik}} \vec{\psi}_i^t \left[\frac{1}{2}\mathbb{P}_{ik}^t\ \vec{V}_i(t_{n+1}) - \frac{1}{2}\mathbb{B}_{ik}\ \vec{\bar{\sigma}}_i(t_{n+\frac{1}{2}})\right] ds \\
&\quad + \sum_{k\in\mathcal{K}(i)} \int_{S_{ik}} \vec{\psi}_i^t \mathbb{P}_{ik}^t\ \vec{V}_i(t_{n+1})\, ds\,. \qquad (90)
\end{aligned}$$

Using Taylor formulae, there exist $c_{n+\frac{1}{2}} \in]t_{n+\frac{1}{2}}, t_{n+1}[$ *and* $d_{n+\frac{1}{2}} \in]t_n, t_{n+\frac{1}{2}}[$ *such that*

$$\vec{V}_h(t_{n+1}) = \vec{V}_h(t_{n+\frac{1}{2}}) + \frac{\Delta t}{2}\partial_t \vec{V}_h(t_{n+\frac{1}{2}}) + \frac{\Delta t^2}{8}\partial_t^2 \vec{V}_h(t_{n+\frac{1}{2}}) + \frac{\Delta t^3}{48}\partial_t^3 \vec{V}_h(c_{n+\frac{1}{2}}), \qquad (91)$$

$$\vec{V}_h(t_n) = \vec{V}_h(t_{n+\frac{1}{2}}) - \frac{\Delta t}{2}\partial_t \vec{V}_h(t_{n+\frac{1}{2}}) + \frac{\Delta t^2}{8}\partial_t^2 \vec{V}_h(t_{n+\frac{1}{2}}) - \frac{\Delta t^3}{48}\partial_t^3 \vec{V}_h(d_{n+\frac{1}{2}}). \qquad (92)$$

On the other hand, applying (89), (91) and (92) in the following equality

$$\int_\Omega \vec{\varphi}_h^t \left(\vec{V}_h(t_{n+1}) - \widehat{\vec{V}_h^{n+1}}\right) dv = \int_\Omega \vec{\varphi}_h^t \left(\vec{V}_h(t_{n+1}) - \vec{V}_h(t_n)\right) dv + \int_\Omega \vec{\varphi}_h^t \left(\vec{V}_h(t_n) - \widehat{\vec{V}_h^{n+1}}\right) dv, \qquad (93)$$

and, by taking into account (50), there exists $e_{n+\frac{1}{2}} \in]t_n, t_{n+\frac{1}{2}}[$ *such that*

$$\begin{aligned}
\int_\Omega \vec{\varphi}_h^t \left(\vec{V}_h(t_{n+1}) - \widehat{\vec{V}_h^{n+1}}\right) dv &= \frac{\Delta t^3}{48} \sum_{i=1}^{N_T} \int_{\mathcal{T}_i} \vec{\varphi}_i^t \left[\partial_t^3 \vec{V}_i(c_{n+\frac{1}{2}}) + \partial_t^3 \vec{V}_i(d_{n+\frac{1}{2}})\right] dv \\
&\quad - \frac{\Delta t^2}{4} \sum_{i=1}^{N_T} \frac{1}{\rho_i} \sum_{k\in\mathcal{E}(i)} \int_{S_{ik}} \vec{\varphi}_i^t \mathbb{A}_{ik} \partial_t \vec{V}_i(e_{n+\frac{1}{2}}) ds\,. \qquad (94)
\end{aligned}$$

Thus, applying the Cauchy-Schwarz inequality and lemma 6, for domains with only free surface boundary conditions (i.e. $\mathcal{E}(i)$ *is empty), there exists a constant* $C > 0$ *such that:*

$$\|\vec{V}_h(t_{n+1}) - \widehat{\vec{V}_h^{n+1}}\|_{\mathrm{L}^2(\Omega)^3} \leq C\Delta t^3 \|\vec{V}_h\|_{\mathrm{C}^3([0,T],\mathrm{L}^2(\Omega)^3)}, \qquad (95)$$

and when the domain has absorbing boundary conditions, we have the following estimate:

$$\|\vec{V}_h(t_{n+1}) - \widehat{\vec{V}_h^{n+1}}\|_{\mathrm{L}^2(\Omega)^3} \leq C\left(\Delta t^3 \|\vec{V}_h\|_{\mathrm{C}^3([0,T],\mathrm{L}^2(\Omega)^3)} + \Delta t^2 \|\vec{V}_h\|_{\mathrm{C}^1([0,T],\mathrm{L}^2(\Omega)^3)}\right). \qquad (96)$$

In the very same way, we obtain analogous estimates for $\|\vec{\bar{\sigma}}_h(t_{n+\frac{3}{2}}) - \widehat{\vec{\bar{\sigma}}_h^{n+\frac{3}{2}}}\|$. *Finally, as* $(\partial_t^3 \vec{V}_h, \partial_t^3 \vec{\bar{\sigma}}_h)$ *is a discrete approximation of* $(\partial_t^3 \vec{V}, \partial_t^3 \vec{\bar{\sigma}})$, *the estimation of the local consistency error is bounded in the following way for unbounded domains or domains with free surface boundary conditions (i.e.* $\mathcal{E}(i)$ *is empty):*

$$\varepsilon_h^n \leq C\Delta t^3 \|(\vec{V}, \vec{\bar{\sigma}})\|_{\mathrm{C}^3([0,T],\mathrm{L}^2(\Omega)^9)}, \qquad (97)$$

and, for domains with absorbing boundary conditions,

$$\varepsilon_h^n \leq C\left(\Delta t^2 \|(\vec{V},\vec{\bar{\sigma}})\|_{\mathrm{C}^1([0,T],\mathrm{L}^2(\Omega)^9)} + \Delta t^3 \|(\vec{V},\vec{\bar{\sigma}})\|_{\mathrm{C}^3([0,T],\mathrm{L}^2(\Omega)^9)}\right). \tag{98}$$

For $(\vec{\varphi}_h,\vec{\psi}_h) \in X_h^1 \times X_h^2$*, we introduce the notations*

$$\mathcal{V}_h^{n+1}(\vec{\varphi}_h) = \sum_{i=1}^{N_T} \mathcal{V}_i^{n+1}(\vec{\varphi}_i) = \sum_{i=1}^{N_T} \int_{\mathcal{T}_i} \rho_i \vec{\varphi}_i^t \frac{\vec{V}_i(t_{n+1}) - \widehat{\vec{V}_i^{n+1}}}{\Delta t}\, dv, \tag{99}$$

$$\mathcal{S}_h^{n+\frac{3}{2}}(\vec{\psi}_h) = \sum_{i=1}^{N_T} \mathcal{S}_i^{n+\frac{3}{2}}(\vec{\psi}_i) = \sum_{i=1}^{N_T} \int_{\mathcal{T}_i} \vec{\psi}_i^t \Lambda_i \frac{\vec{\bar{\sigma}}_i(t_{n+\frac{3}{2}}) - \widehat{\vec{\bar{\sigma}}_i^{n+\frac{3}{2}}}}{\Delta t}\, dv, \tag{100}$$

which, combined with (97) for unbounded domains or domains with free surface boundary conditions, lead to

$$|||\mathcal{V}_h^{n+1}||| + |||\mathcal{S}_h^{n+\frac{3}{2}}||| \leq C\Delta t^2 \|(\vec{V},\vec{\bar{\sigma}})\|_{\mathrm{C}^3([0,T],\mathrm{L}^2(\Omega)^9)}; \tag{101}$$

using (98) for absorbing boundary conditions, it holds

$$|||\mathcal{V}_h^{n+1}||| + |||\mathcal{S}_h^{n+\frac{3}{2}}||| \leq C\left(\Delta t \|(\vec{V},\vec{\bar{\sigma}})\|_{\mathrm{C}^1([0,T],\mathrm{L}^2(\Omega)^9)} + \Delta t^2 \|(\vec{V},\vec{\bar{\sigma}})\|_{\mathrm{C}^3([0,T],\mathrm{L}^2(\Omega)^9)}\right), \tag{102}$$

where we denote by $|||.|||$ *the norm of the linear forms on* $\mathrm{L}^2(\Omega)^3$ *or* $\mathrm{L}^2(\Omega)^6$*.*

On the other hand, according to (89) and (90), the semi-discrete solution $(\vec{V}_h,\vec{\bar{\sigma}}_h) \in \mathrm{C}^1([0,T], X_h^1 \times X_h^2)$ *verifies:*

$$\begin{aligned}
\rho_i \int_{\mathcal{T}_i} \vec{\varphi}_i^t \frac{\vec{V}_i(t_{n+1}) - \vec{V}_i(t_n)}{\Delta t}\, dv &= -\sum_{\alpha\in\{x,y,z\}} \int_{\mathcal{T}_i} (\partial_\alpha \vec{\varphi}_i)^t \mathbb{M}_\alpha \vec{\bar{\sigma}}_i(t_{n+\frac{1}{2}})\, dv \\
&\quad + \sum_{k\in\mathcal{V}(i)} \int_{S_{ik}} \vec{\varphi}_i^t \mathbb{P}_{ik} \frac{\vec{\bar{\sigma}}_i(t_{n+\frac{1}{2}}) + \vec{\bar{\sigma}}_k(t_{n+\frac{1}{2}})}{2}\, ds \\
&\quad + \sum_{k\in\mathcal{E}(i)} \int_{S_{ik}} \vec{\varphi}_i^t \left[\frac{1}{2}\mathbb{P}_{ik}\ \vec{\bar{\sigma}}_i(t_{n+\frac{1}{2}}) - \frac{1}{2}\mathbb{A}_{ik}\ \vec{V}_i(t_n)\right]\, ds + \mathcal{V}_i^{n+1}(\vec{\varphi}_i)\,, \qquad (103) \\
\int_{\mathcal{T}_i} \vec{\psi}_i^t \Lambda_i \frac{\vec{\bar{\sigma}}_i(t_{n+\frac{3}{2}}) - \vec{\bar{\sigma}}_i(t_{n+\frac{1}{2}})}{\Delta t}\, dv &= -\sum_{\alpha\in\{x,y,z\}} \int_{\mathcal{T}_i} (\partial_\alpha \vec{\psi}_i)^t \mathbb{M}_\alpha^t \vec{V}_i(t_{n+1}) dv \\
&\quad + \sum_{k\in\mathcal{V}(i)} \int_{S_{ik}} \vec{\psi}_i^t \mathbb{P}_{ik}^t \frac{\vec{V}_i(t_{n+1}) + \vec{V}_k(t_{n+1})}{2} ds \\
&\quad + \sum_{k\in\mathcal{E}(i)} \int_{S_{ik}} \vec{\psi}_i^t \left[\frac{1}{2}\mathbb{P}_{ik}^t\ \vec{V}_i(t_{n+1}) - \frac{1}{2}\mathbb{B}_{ik}\ \vec{\bar{\sigma}}_i(t_{n+\frac{1}{2}})\right] ds \\
&\quad + \sum_{k\in\mathcal{K}(i)} \int_{S_{ik}} \vec{\psi}_i^t \mathbb{P}_{ik}^t\ \vec{V}_i(t_{n+1})\ ds + \mathcal{S}_i^{n+\frac{3}{2}}(\vec{\psi}_i)\,. \qquad (104)
\end{aligned}$$

Finally, using (26)-(103) and (27)-(104), the field $(\mathscr{V}_h^n, \mathscr{S}_h^{n+\frac{1}{2}}) = (\vec{V}_h(t_n) - \vec{V}_h^n, \vec{\bar{\sigma}}_h(t_{n+\frac{1}{2}}) - \vec{\bar{\sigma}}_h^{n+\frac{1}{2}})$ *satisfies the*

following set of equations:

$$\begin{aligned}
\rho_i \int_{\mathcal{T}_i} \vec{\varphi}_i^t \frac{\mathscr{V}_i^{n+1} - \mathscr{V}_i^n}{\Delta t}\, dv &= -\sum_{\alpha\in\{x,y,z\}} \int_{\mathcal{T}_i} (\partial_\alpha \vec{\varphi}_i)^t \mathbb{M}_\alpha \mathscr{S}_i^{n+\frac{1}{2}}\, dv \\
&\quad + \sum_{k\in\mathcal{V}(i)} \int_{S_{ik}} \vec{\varphi}_i^t \mathbb{P}_{ik} \frac{\mathscr{S}_i^{n+\frac{1}{2}} + \mathscr{S}_k^{n+\frac{1}{2}}}{2}\, ds \\
&\quad + \sum_{k\in\mathcal{E}(i)} \int_{S_{ik}} \vec{\varphi}_i^t \left[\frac{1}{2}\mathbb{P}_{ik}\ \mathscr{S}_i^{n+\frac{1}{2}} - \frac{1}{2}\mathbb{A}_{ik}\ \mathscr{V}_i^n\right] ds + \mathcal{V}_i^{n+1}(\vec{\varphi}_i)\,, \qquad (105) \\
\int_{\mathcal{T}_i} \vec{\psi}_i^t \Lambda_i \frac{\mathscr{S}_i^{n+\frac{3}{2}} - \mathscr{S}_i^{n+\frac{1}{2}}}{\Delta t}\, dv &= -\sum_{\alpha\in\{x,y,z\}} \int_{\mathcal{T}_i} (\partial_\alpha \vec{\psi}_i)^t \mathbb{M}_\alpha^t \mathscr{V}_i^{n+1} dv \\
&\quad + \sum_{k\in\mathcal{V}(i)} \int_{S_{ik}} \vec{\psi}_i^t \mathbb{P}_{ik}^t \frac{\mathscr{V}_i^{n+1} + \mathscr{V}_k^{n+1}}{2} ds \\
&\quad + \sum_{k\in\mathcal{E}(i)} \int_{S_{ik}} \vec{\psi}_i^t \left[\frac{1}{2}\mathbb{P}_{ik}^t\ \mathscr{V}_i^{n+1} - \frac{1}{2}\mathbb{B}_{ik}\ \mathscr{S}_i^{n+\frac{1}{2}}\right] ds \\
&\quad + \sum_{k\in\mathcal{K}(i)} \int_{S_{ik}} \vec{\psi}_i^t \mathbb{P}_{ik}^t\ \mathscr{V}_i^{n+1}\ ds + \mathcal{S}_i^{n+\frac{3}{2}}(\vec{\psi}_i)\,. \qquad (106)
\end{aligned}$$

Now, we introduce the error energy $\mathscr{E}^n$ at time $n\Delta t$ by:

$$\begin{aligned}
\mathscr{E}^n &= \frac{1}{2}\sum_{i=1}^{N_T} \int_{\mathcal{T}_i} \left[\rho_i \left(\mathscr{V}_i^n\right)^t \mathscr{V}_i^n + \left(\mathscr{S}_i^{n+\frac{1}{2}}\right)^t \Lambda_i\ \mathscr{S}_i^{n-\frac{1}{2}}\right] dv \\
&\quad - \frac{\Delta t}{8}\sum_{i=1}^{N_T}\sum_{k\in\mathcal{E}(i)} \int_{S_{ik}} \left[\left(\mathscr{V}_i^n\right)^t \mathbb{A}_{ik}\ \mathscr{V}_i^n - \left(\mathscr{S}_i^{n-\frac{1}{2}}\right)^t \mathbb{B}_{ik}\ \mathscr{S}_i^{n-\frac{1}{2}}\right] ds. \qquad (107)
\end{aligned}$$

Reasoning similarly as for the discrete corrected energy, we can prove that under a CFL condition of the same type as (38), we have for domains with free surface boundary conditions only:

$$\left(\|\mathscr{V}_h^n\|^2_{\mathrm{L}^2(\Omega)^3} + \|\mathscr{S}_h^{n+\frac{1}{2}}\|^2_{\mathrm{L}^2(\Omega)^6}\right)^{1/2} \leq C\Delta t^2 \|(\vec{V},\vec{\tilde{\sigma}})\|_{\mathrm{C}^3([0,T],\mathrm{L}^2(\Omega)^9)} \qquad (108)$$

and, for absorbing boundary conditions, we obtain

$$\left(\|\mathscr{V}_h^n\|^2_{\mathrm{L}^2(\Omega)^3} + \|\mathscr{S}_h^{n+\frac{1}{2}}\|^2_{\mathrm{L}^2(\Omega)^6}\right)^{1/2} \leq C\left(\Delta t \|(\vec{V},\vec{\tilde{\sigma}})\|_{\mathrm{C}^1([0,T],\mathrm{L}^2(\Omega)^9)} + \Delta t^2 \|(\vec{V},\vec{\tilde{\sigma}})\|_{\mathrm{C}^3([0,T],\mathrm{L}^2(\Omega)^9)}\right). \qquad (109)$$

Finally, we can conclude that the order of convergence of the scheme is $\mathcal{O}(\Delta t^\alpha + h^{\min(s,k)})$ by using the triangular inequality and results already established in the semi-discrete case (see Th. 2):

$$\begin{aligned}
&\max_{n=0,\ldots,N} \left(\|\vec{V}(t_n) - \vec{V}_h^n\|^2_{\mathrm{C}^0([0,T],\mathrm{L}^2(\Omega)^3)} + \|\vec{\tilde{\sigma}}(t_{n+\frac{1}{2}}) - \vec{\tilde{\sigma}}_h^{n+\frac{1}{2}}\|^2_{\mathrm{C}^0([0,T],\mathrm{L}^2(\Omega)^6)}\right)^{1/2} \qquad (110) \\
\leq\ & C\Delta t^\alpha \|(\vec{V},\vec{\tilde{\sigma}})\|_{\mathrm{C}^{2\alpha-1}([0,T],\mathrm{L}^2(\Omega)^9)} + Ch^{\min(s,k)} \|(\vec{V},\vec{\tilde{\sigma}})\|_{\mathrm{C}^0([0,T],P\mathrm{H}^{s+1}(\Omega)^9)} \qquad (111) \\
\leq\ & C(\Delta t^\alpha + h^{\min(s,k)}) \left(\|(\vec{V},\vec{\tilde{\sigma}})\|_{\mathrm{C}^{2\alpha-1}([0,T],\mathrm{L}^2(\Omega)^9)} + \|(\vec{V},\vec{\tilde{\sigma}})\|_{\mathrm{C}^0([0,T],P\mathrm{H}^{s+1}(\Omega)^9)}\right), \qquad (112)
\end{aligned}$$

where $\alpha = 1$ if the absorbing boundary conditions are invocated, otherwise $\alpha = 2$ for domains with free surface boundary conditions only.

6 Numerical results

The numerical method has been applied to two different studies. First, the propagation of an eigenmode in three dimensions of space allows a convergence study of the scheme in the case of uniform and non uniform meshes. The second application concerns the propagation of the wave produced by an explosive source in a half-space which enables validating source introduction and absorbing boundary conditions and a study of the accuracy of the method in a more realistic context.

6.1 Convergence study: propagation of an eigenmode in 3D

The first problem concerns the propagation of an eigenmode in three dimensions of space. The domain of computation is the unit cubic cavity on which we apply free surface boundary conditions. We are interested in the $(1,1,1)$ mode whose exact solution at time t and in $X=(x,y,z)$ is given by:

$$\left\{\begin{array}{rcl} V_x(t,X) &=& \cos(\pi x)\ [\sin(\pi y)-\sin(\pi z)]\ \cos(\Omega t)\,, \\ V_y(t,X) &=& \cos(\pi y)\ [\sin(\pi z)-\sin(\pi x)]\ \cos(\Omega t)\,, \\ V_z(t,X) &=& \cos(\pi z)\ [\sin(\pi x)-\sin(\pi y)]\ \cos(\Omega t)\,, \\ \sigma_{xx}(t,X) &=& -A\ \sin(\pi x)\ [\sin(\pi y)-\sin(\pi z)]\ \sin(\Omega t)\,, \\ \sigma_{yy}(t,X) &=& -A\ \sin(\pi y)\ [\sin(\pi z)-\sin(\pi x)]\ \sin(\Omega t)\,, \\ \sigma_{zz}(t,X) &=& -A\ \sin(\pi z)\ [\sin(\pi x)-\sin(\pi y)]\ \sin(\Omega t)\,, \\ \sigma_{xy}(t,X) &=& \sigma_{xz}=\sigma_{xz}=0\,, \end{array}\right. \tag{113}$$

with $A=\sqrt{2\,\rho\,\mu}$ and $\Omega=\pi\sqrt{2\mu/\rho}$. We set dimensionless values for the medium properties, $\rho=1.0$, $\lambda=0.5$ and $\mu=0.25$, which implies that v_p=1. and v_s=0.5. The initialisation of the leap-frog scheme is realized by deducing from the analytical expressions (113) the values at $t=0$ for the velocity components and at $t=\frac{\Delta t}{2}$ for the stress components. The L^2-error at step n between the exact value and the solution of the numerical scheme in the unit cube depends on velocities V_α $(\alpha=x,y,z)$ at $t=n\Delta t$ and stresses $\sigma_{\alpha\beta}$ $(\alpha,\beta=x,y,z)$ at $t=(n+\frac{1}{2})\Delta t$ and writes

$$err^n_{\mathrm{L}^2}=\sqrt{\sum_{i=1}^{N_T}\int_{\mathcal{T}_i}\left[\sum_{\alpha\in\{x,y,z\}}\left(V_\alpha(n\Delta t,X_i)-(V_\alpha)^n_i\right)^2+\sum_{\alpha,\beta\in\{x,y,z\}}\left(\sigma_{\alpha\beta}\left(\left(n+\frac{1}{2}\right)\Delta t,X_i\right)-(\sigma_{\alpha\beta})^{n+1/2}_i\right)^2\right]dv\,.}$$

Series of different uniform and non uniform meshes have been constructed for a numerical study of the convergence of the scheme. Different methods have been used, the notation P_k refering to a scheme based on polynomials of degree k. Uniform meshes are obtained by dividing the domain in cubic cells which are split in six tetrahedra. On the other hand, the non uniform meshes are constructed using the three-dimensional mesh generator GMSH [16] and the different meshes are obtained by successive refinements of an initial coarse mesh. Three of them are presented in figure 1. For both types of meshes, the mesh spacing h is the length of the longest edge of the mesh (i.e. h_{max}). The characteristics of both uniform and non uniform meshes are given in table 1.

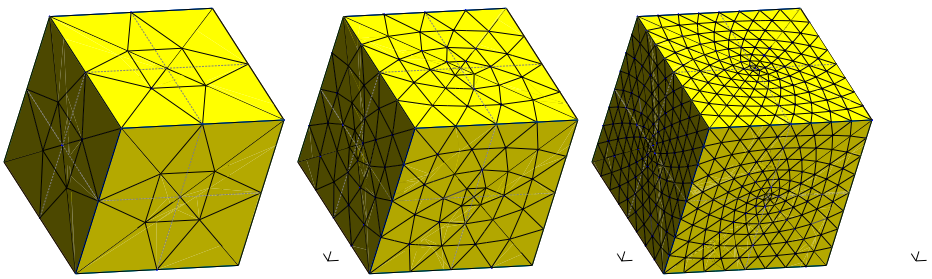

Figure 1: Non uniform meshes M2, M3 and M4.

On both figures 2 and 3, we display the numerical error, at time t=5.0s, in L^2-norm and in logarithmic scale, by respect to the mesh spacing h_{max} (left picture) and by respect to the corresponding CPU time (right picture). Figure 2 is concerned with uniform meshes whereas figure 3 refers to non uniform meshes. For uniform and non uniform meshes, we observe a convergence approximatively of order k for a method P_k, which proves the

Uniform meshes				
Mesh	h_{min}	h_{max}	N_N	N_T
M1	0.5	0.866	27	48
M2	0.25	0.433	125	384
M3	0.125	0.216	729	3 072
M4	$6.25\ 10^{-2}$	0.108	4 913	24 576
M5	$3.125\ 10^{-2}$	$5.412\ 10^{-2}$	35 937	196 608

Non uniform meshes				
Mesh	h_{min}	h_{max}	N_N	N_T
M1	0.707	1.0	14	24
M2	0.234	0.520	70	227
M3	$8.21\ 10^{-2}$	0.293	398	1 715
M4	$2.90\ 10^{-2}$	0.193	2 400	11 899
M5	$1.03\ 10^{-2}$	$9.52\ 10^{-2}$	17 993	98 309

Table 1: Characteristics of the uniform and non uniform meshes used for the convergence study ; N_N and N_T are respectively the number of nodes and tetrahedra of the meshes.

enhancement provided by higher degree methods. Note that this study also proves that the free surface condition is accurately discretized, as proved in the previous section. If we examine the efficiency, we notice that, to obtain a given L^2-error, methods based on high degree polynomials need lower CPU times, for both types of meshes. We also remark the good behavior of the method for non uniform meshes, since CPU times necessary to reach a given error level are comparable to times corresponding to uniform meshes. So, we can conclude that, for this test case, higher order approximations are more accurate and more efficient for both type of meshes.

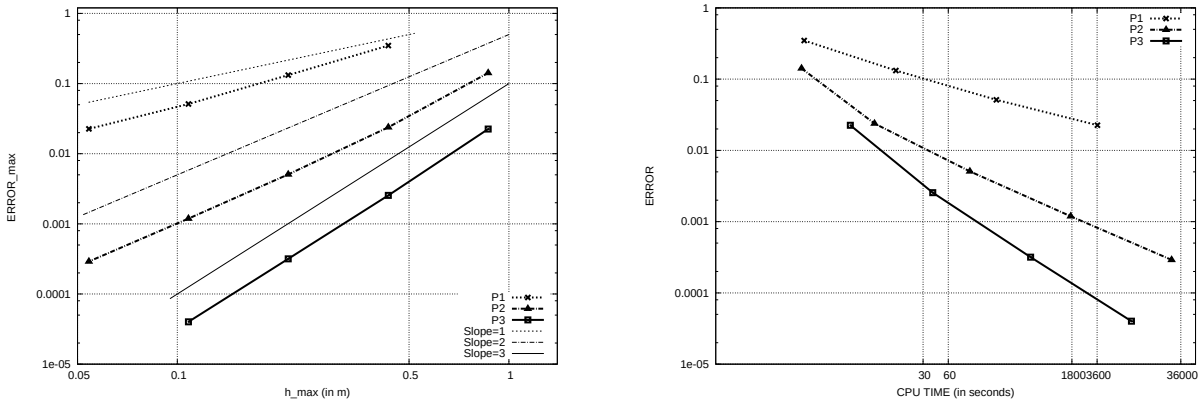

Figure 2: Convergence and CPU time for the (1,1,1) eigenmode at $t = 5.0$s on uniform meshes.

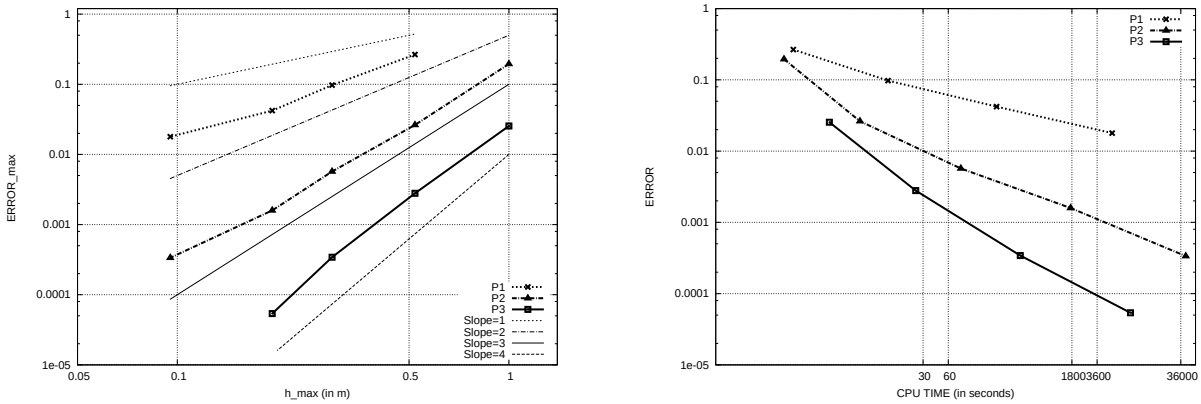

Figure 3: Convergence and CPU time for the (1,1,1) eigenmode at $t = 5.0$s on non uniform meshes.

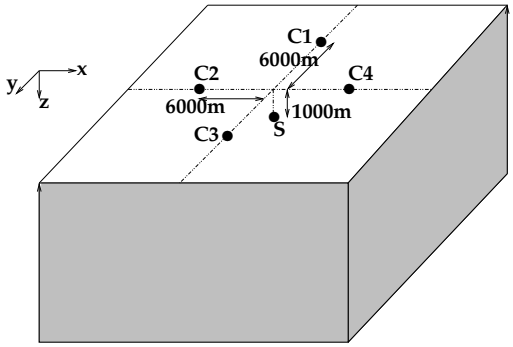

Figure 4: Explosive source in a half-space. Position of the source S and the four surface sensors.

6.2 Explosive source in a half-space

The method has also been applied to a more realistic test case i.e. the propagation of the wave produced by an explosive source in a homogeneous half-space, as illustrated in figure 4, allowing the validation of the source implementation and the absorbing boundary conditions.

The medium is homogeneous of density ρ=2800 kg/m^3 and P- and S- waves velocities are respectively v_p=6400 m/s and v_s=3700 m/s. We apply a free surface condition on the upper boundary of the domain and absorbing conditions on the other boundaries. The source is located at the center of the domain at 1000m depth (at the coordinates (0;0;1000)) and four surface sensors are placed at 6000m from the epicenter, symmetrically on the x- and y-axis, as described in figure 4. The source signal is a Ricker wavelet whose moment-rate is given by

$$s(t) = \frac{3.10^{16}}{\alpha\sqrt{\pi}}\, exp\left[-\frac{(t-1)^2}{\alpha^2}\right] \tag{114}$$

with α=0.25, corresponding to a central frequency equal to f_c =1.0Hz and a maximum frequency of f_{max} =3.0Hz. Thus, the wavelength $L = v_s/f_{max}$ is approximatively equal to 1233m. The explosive source is introduced as a right hand side on the diagonal components of the stress tensor i.e. for σ_{xx}, σ_{yy} and σ_{zz}. In order to compare the results obtained when using several methods P_k, notably the finite volume method (P_0), this right hand side writes $s(t)\, g(x,y,z)$ where g is defined by

$$g(x,y,z) = \frac{1}{M}\, exp\left[-\frac{(x-x_S)^2+(y-y_S)^2+(z-z_S)^2}{h^2}\right] \quad \text{with} \quad M = \int_\Omega g(x,y,z)\, dv\,,$$

where (x_S, y_S, z_S) are the source coordinates. Note that the support of g is taken sufficiently small, compared to the element size, for an accurate approximation of a point source, a right hand side based on a Dirac function $s(t)\,\delta(x_S, y_S, z_S)$ being only compatible with high degree approximation based methods. Initial conditions for the system are $\vec{V} = \vec{0}$ and $\vec{\sigma} = \vec{0}$ and solutions are calculated until time t=6.0s.

The calculation domain is 36km×36km×12km. Solutions have been obtained using several uniform tetrahedral meshes constructed, as previously for the eigenmode test case, by dividing the domain in cubic cells of edge h which are split in six tetrahedra. The mesh spacing h, i.e. here the smallest edge of the mesh, can be expressed as a function of the wavelength L as summarized in table 2. Calculations have been performed on 64 processors using

h (in meters)	400	300	200	150	100	75
Approx. L/n	$L/3$	$L/4$	$L/6$	$L/8$	$L/12$	$L/16$
Nb. tetrahedra	1 458 000	3 456 000	11 664 000	27 648 000	93 312 000	221 184 000
Nb. tetra./proc.	22 781	54 000	182 250	432 000	1 458 000	3 456 000

Table 2: Correspondance between the mesh spacing h and the wavelength L of the source function. Characteristics of the different meshes (total number of tetrahedra, number of tetrahedra for each processor).

Message Passing Interface (MPI), whatever the mesh spacing, for a better comparison of the CPU times between the different methods. The characteristics of the different meshes are also listed in table 2.

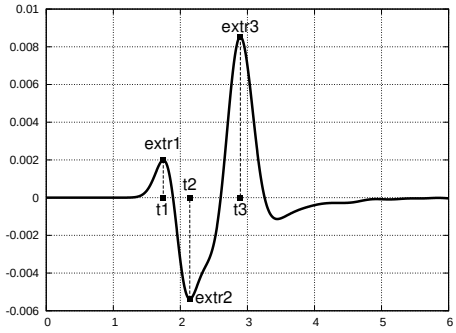

Figure 5: Velocity V_z (m/s) as a function of time (s) ; reference solution at sensor 1. Extrema and corresponding times for the evaluation of errors err_2 and err_3.

For such a test case where no exact solution is available, we have to define some criteria in order to estimate very meticulously the accuracy of the solution. Firstly, we check two particular properties, consequences of an explosive source, which are i) V_x=0 at sensors C1 and C3 (on y-axis) and V_y=0 at sensors C2 and C4 (on x-axis) and ii) the evolution at the surface of the vertical velocity component V_z only depends on the distance to the epicenter, thus the V_z profiles obtained at the four sensors are superimpose. Moreover, for a validation of the source introduction, the amplitudes and the travel times of the computed profiles are compared to a reference solution computed at these four sensors (and not everywhere in the computational domain) using the Discrete Wave Number method [6]. Then, three different errors are defined. First, err_1 is concerned with the components which are ideally equal to zero and expresses

$$err_1 = \max_{t\in[0.;6.]} \left[|V_x|_{C_1}, |V_y|_{C_2}, |V_x|_{C_3}, |V_y|_{C_4} \right] .$$

The two other errors depend on the values at the extrema, as illustrated in figure 5. For each non null velocity profile (for instance, here, V_z for the reference solution at sensor 1), we identify three extrema and note their values ($V_z(extr_i)$, i=1,2,3) and the corresponding times (t_i, i=1,2,3).

From these data, we define a relative error, in the amplitude or in time, between two profiles (for instance profiles at sensors C_j and C_k), for a given velocity component V_α and a given extremum $extr_i$ by the following formulae, for amplitudes and times

$$err_{rel}\left(V_\alpha, C_j/C_k, extr_i\right)_{ampl} = \left| \frac{V_\alpha(extr_i)_{C_j} - V_\alpha(extr_i)_{C_k}}{V_\alpha(extr_i)_{ref}} \right| ,$$

$$err_{rel}\left(V_\alpha, C_j/C_k, extr_i\right)_{t} = \left| \frac{t_{i/C_j} - t_{i/C_k}}{t_{i/ref}} \right| ,$$

where the subscript *ref* stands for the corresponding value of the reference solution. Thus, error err_2 measures the asymmetries of the computed solution (i.e. the mean maximum error of the amplitude and the travel time between solutions computed at two sensors) of the vertical velocity component V_z which writes

$$err_{2/ampl} = \frac{1}{3}\sum_{i=1}^{3} \max_{1\le j,k\le 4} err_{rel}\left(V_z, C_j/C_k, extr_i\right)_{ampl} ,$$

$$err_{2/t} = \frac{1}{3}\sum_{i=1}^{3} \max_{1\le j,k\le 4} err_{rel}\left(V_z, C_j/C_k, extr_i\right)_{t} .$$

Finally, err_3 is the mean error between the computed and the reference solutions at all sensors, for all non null velocity components and for all extrema. This error writes, for instance for amplitudes

$$err_{3/ampl} = \frac{1}{24}\sum_{i=1}^{3} \left[\sum_{j\in\{2,4\}} err_{rel}\left(V_x, C_j/C_{j/ref}, extr_i\right)_{ampl} + \right.$$
$$\left. \sum_{j\in\{1,3\}} err_{rel}\left(V_y, C_j/C_{j/ref}, extr_i\right)_{ampl} + \sum_{j=1}^{4} err_{rel}\left(V_z, C_j/C_{j/ref}, extr_i\right) \right] ,$$

an equivalent definition being applied to define $err_{3/t}$ on times.

Calculations have been done using methods based on different degrees of interpolation in combination with the meshes defined in table 2 in order to study the convergence and CPU time corresponding to the three types of errors; the results of these calculations are gathered in figure 6 and the CPU time of each calculation is given in table 3. Note that, as previously, P_k refers to a method based on polynomials of degree k.

The first line of the figure presents the values of err_1 as a function of the mesh spacing h (left picture) and by respect to the corresponding CPU time (right picture). When examining these results, we notice (left picture) that err_1 corresponding to P_0 method remains nearly constant, whatever the mesh spacing, in the order of 10% of the maximum value of the velocity. Results are clearly improved by the use of higher degree methods since, in comparison with the P_0 results, the value of the P_2 method is reduced by a factor 10^3. Moreover, higher degree methods P_2 and P_3 are also more efficient since a given error level of accuracy is obtained for lower CPU times.

Now, we study the second line of figures corresponding to err_2, which is a relative error traducing the asymmetry of the V_z profiles by respect to h (left picture) and the CPU time (right picture). As previously, we notice that the results of the P_0 method are not accurate enough even using the finest meshes. The improvement on the symmetry is obvious when using the other methods, especially the P_2 and P_3 methods resulting in err_2 values lower than 0.1%. As previously for err_1, P_2 and P_3 are the two most efficient methods.

Finally, we analyse the results obtained for err_3 (last line of figure 6) which is a relative error between the computed and the reference solutions at the extrema. As previously, the lowest error levels correspond to the P_2 and P_3 methods whereas the P_0 method produces relative errors in the order of 10% and this independently on h. The other methods allow errors lower than 5% when using the finest meshes. Note that, for this last error, if the improvement between P_0 and P_1 is obvious, it is more limited for the two highest degree methods. Furthermore, the P_2 and P_3 methods lead to the same level of error. This fact is also visible when err_3 is plotted as a function of the CPU time (right picture). The improvement on the error levels for the P_2 and P_3 methods is not sufficient to compensate their overcost; thus, for this last error, the P_1 method appears to be most efficient.

	CPU (s)					
P_k/h	400	300	200	150	100	75
P_0		1min 18s	7min	18min	1h 28min	4h 31min
P_1		17min	1h 14min	3h 40min	18h 23min	65h 34min
P_2	38min	1h 44min	8h 12min	25h 20min		
P_3	3h	8h 07min	39h 50 min			

Table 3: CPU times of the calculations for the P_k methods and the different meshes on 64 processors.

We also present, in figure 7, the errors $err_{2/t}$ (left picture) and $err_{3/t}$ (right picture) on travel times as a function of the mesh spacing. From the study of $err_{2/t}$, we firstly notice a clear difference between P_0 and other methods. Relative error on time is approximatively 0.01% for the P_2 and P_3 methods which is negligible, about 0.1% for the P_1 method and greater than 1% for the P_0 method. We remark a comparable behaviour on $err_{3/t}$ and values about 0.5% for the P_2 and P_3 methods.

In conclusion of this study, we have to distinguish results obtained with the P_0 method from those of the other methods P_k (k=1,2,3). First of all, the P_0 method leads to the worst levels of errors, for amplitudes and travel times, and the use of fine meshes do not allow improving these results. Moreover, when combining the different criteria on the solution, the P_2 seems to represent the better compromise between accuracy and efficiency.

The results obtained, at sensor 1, with the method P_2 and a mesh spacing h=200m are presented in figure 8. They are also compared to the reference solution. This constitutes a validation of the source implementation and of the absorbing boundary conditions since no spurious reflections from the boundaries appear in the profiles.

7 Conclusion

We proposed a discontinuous Galerkin finite element method to solve the first-order hyperbolic system of the elastodynamic equations, written in velocity-stress formulation. This method is applied to non uniform tetraedral meshes allowing an accurate approximation of the medium or mesh refinement in particular areas of the domain. The spatial approximation is based on high degree polynomials defined locally on each element of the mesh. The scheme combines centered fluxes and a leap-frog scheme in time which leads to a non diffusive method. We also detailed a simple absorbing boundary condition, derived from an upwind scheme. In this paper, the properties of

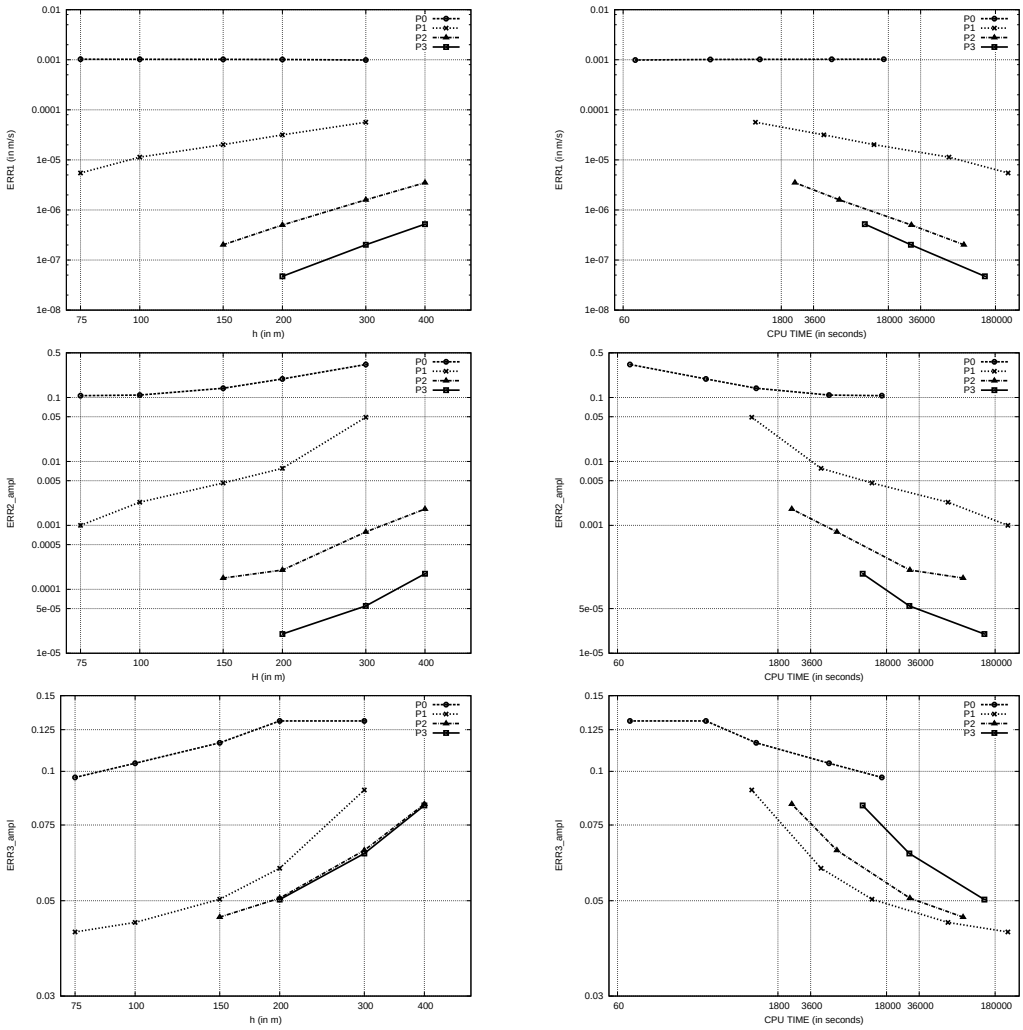

Figure 6: Convergence and CPU time for errors err_1 (first line of figures), err_2 (second line of figures) and err_3 (last line of figures) on amplitudes. Explosive source in a half-space, solutions at t =6.s, uniform meshes, computations on 64 processors.

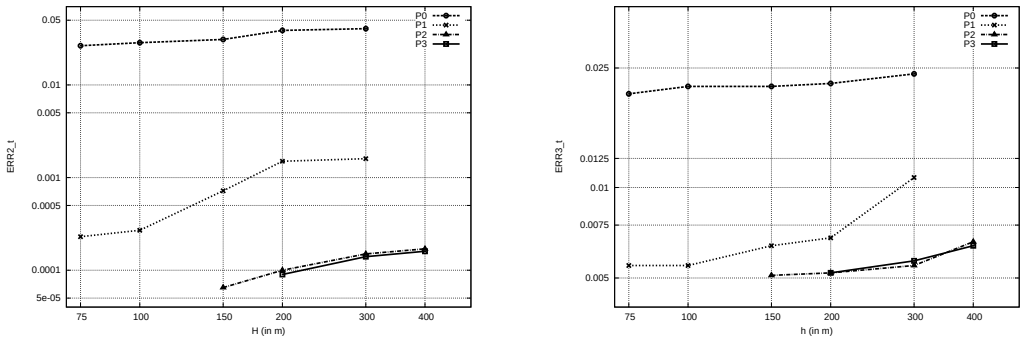

Figure 7: Convergence of $err_{2/t}$ (left picture) and $err_{3/t}$ (right picture) on travel times. Explosive source in a half-space, solutions at t =6.s, uniform meshes, computations on 64 processors.

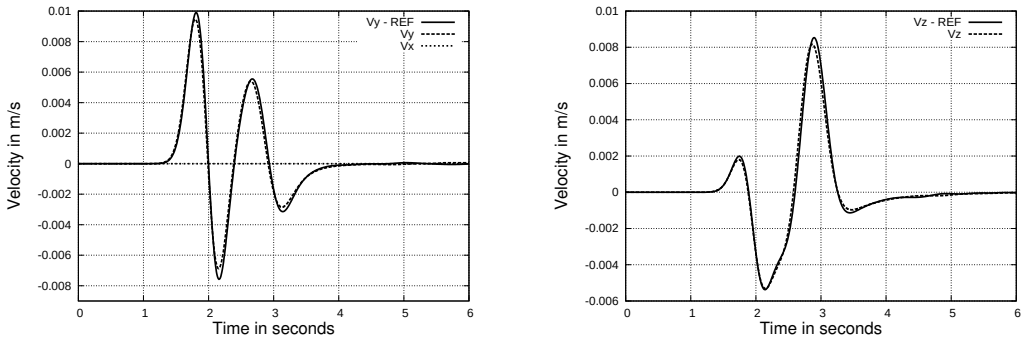

Figure 8: Comparison between computed and reference solutions at sensor 1. V_x and V_y (left picture) and V_z (right picture). Computed solution corresponds to P_2 method for a mesh spacing equal to 200m.

the method have been analysed in detail. First, we have proved that this explicit scheme is stable under a CFL type condition resulting from a discrete energy which is preserved in domains with free surfaces and decreasing in presence of absorbing boundary conditions. Moreover, the convergence of the method for the semi-discrete and the fully discrete schemes has been studied. More precisely, for solutions regular enough, the scheme is convergent with an order $\mathcal{O}(\Delta t^\alpha + h^k)$, where k is the degree of the polynomial approximation, and $\alpha = 2$ for domains with only free surface boundary conditions, or $\alpha = 1$ when the absorbing boundary conditions are included in the scheme.

Three-dimensional numerical results have been obtained with a parallel implementation of the DG method. The first one refers to the propagation of an eigenmode in a cubic cavity for which an exact solution is known and a numerical study of the convergence has been realised for series of uniform and non uniform meshes. The second test case concerns a more realistic problem i.e. the propagation of the waves due to an explosion in a half-space involving the validation of the source implementation and the absorbing boundary conditions. The main conclusions of this study are the accuracy and the efficiency of the method particularly for higher degree polynomial interpolations. These results highlight the gain obtained with these methods, especially when compared to the finite volumes method (P0) for which mesh refinement did not enable improving both errors on amplitudes and travel time. The better compromise between accuracy and CPU time seems obtained using the P2 method (based on polynomials of degree 2). Moreover, the free surface condition is accurately approximated. These results are encouraging and could be developed in several interesting directions. First, the treatment at absorbing boundaries could be improved using more accurate boundary conditions. Many techniques have been proposed to reduce spurious reflections, including additional absorbing layers which may be costly in 3D. Then, high-order non reflecting boundary conditions [15] or an implicit treatment of our simple absorbing condition could be interesting ways of improvement. Secondly, the global accuracy of the 3D method could be increased by the use of a fourth-order leap-frog scheme in time, as done in [17] for 2D elastic wave propagation, leading to high-order methods in both space and time with the ability to use coarser meshes. Finally, we are interested in simulations of more realistic three dimensional problems including topography and realistic media. Thus, the extension of this scheme to viscoelastic rheologies is on the way.

References

[1] P.F. Antonietti, I. Mazzieri, A. Quarteroni and F. Rapetti, *Non-conforming high order approximations of the elastodynamics equation*, Comput. Methods Appl. Mech. Engrg, 209–212, pp 212–238, 2012.

[2] S. Aoi and H. Fujiwara, *3D Finite-difference method using discontinuous grids*, Bull. Seism. Soc. Am., 89, pp 918–930, 1999.

[3] Z. Alterman and F.C. Karal, *Propagation of elastic waves in layered media by finite-difference methods*, Bull. Seism. Soc. Am., 58, 367–398, 1968.

[4] H. Bao, J. Bielak, O. Ghattas, L. Kallivokas, D.R. O'Hallaron, J.R. Schewchuk and J. Xu, *Large-scale simulation of elastic wave propagation in heterogeneous media on parallel computers*, Computer Methods in Applied Mechanics and Engineering, 152, pp 85–102, 1998.

[5] A. Bayliss, K.E. Jordan, B.J. LeMesurier and E. Turkel, *A fourth-order accurate finite-difference scheme for the computation of elastic waves*, Bull. Seism. Soc. Am., 76, pp 1115–1132, 1986.

[6] M. Bouchon and K. Aki, *Discrete wave-number representation of seismic-source wave fields*, Bull. Seism. Soc. Am., 67, pp 259–277, 1977.

[7] M. Benjemaa, S. Piperno and N. Glinsky-Olivier, *Etude de stabilité d'un schéma volumes finis pour les équations de l'élasto-dynamique en maillages non structurés*, INRIA report 5817, 2006.

[8] M. Benjemaa, *Etude et simulation numérique de la rupture dynamique des séismes par des méthodes d'éléments finis discontinus*, Ph.D. thesis Nice-Sophia Antipolis University, 2007.

[9] E. Chaljub, Y. Capdeville and J.P. Vilotte *Solving elastodynamics in a fluid–solid heterogeneous sphere: a parallel spectral element approximation on non–conforming grids*, J. Comp. Phy., 187,2 pp 457–491, 2003.

[10] P. Ciarlet, *The finite element method for elliptic problems*, North Holland-Elsevier science publishers, Amsterdam, New York, Oxford, 1978.

[11] S. Delcourte, L. Fezoui and N. Glinsky-Olivier, *A high-order Discontinuous Galerkin method for the seismic wave propagation*, ESAIM Proc., 27, pp 70–89, 2009.

[12] M. Dumbser and M. Käser, *An arbitrary high-order Discontinuous Galerkin method for elastic waves on unstructured meshes II: the three-dimensional isotropic case*, Geophysical J. Int., 167(1), pp 319–336, 2006.

[13] L. Fezoui, S. Lanteri, S. Lohrengel and S. Piperno, *Convergence and stability of a Discontinuous Galerkin time-domain method for the 3D heterogeneous Maxwell equations on unstructured meshes*, M2AN, 39 (6), pp 1149–1176, 2005.

[14] M. Galis, P. Moczo and J. Kristek, *A 3-D hybrid finite-difference–finite-element viscoelastic modelling of seismic wave motion*, Geophys. J. Int., 175, pp 153–184, 2008.

[15] D. Givoli, *High-order local non-reflecting boundary conditions: a review*, Wave Motion, 39, pp 319–326, 2004.

[16] C. Geuzaine and J.F. Remacle, *Gmsh: a three-dimensional finite element mesh generator with buit-in-pre and post-processing facilities*, Int. J. Numer. Meth. Engng, 11, pp 1309–1331, 2009.

[17] N. Glinsky, S. Moto Mpong and S. Delcourte, *A high-order discontinuous Galerkin scheme for elastic wave propagation*, INRIA report, nř7476, 2010.

[18] M. Käser, V. Hermann and J. de la Puente, *Quantitative accuracy analysis of the discontinuous Galerkin method for seismic wave propagation*, Geophys. J. Int., 173(2), pp 990-999, 2008.

[19] K.R. Kelly, R.W. Ward, S. Treitel and R.M. Alford, *Synthetic seismograms : a finite-difference approach*, Geophysics, 41, pp 2–27, 1976.

[20] D. Komatitsch and J.P. Vilotte, *The spectral-element method: an efficient tool to simulate the seismic response of 2D and 3D geological structures*, Bull. Seism. Soc. America, 88 (2), pp 368–392, 1998.

[21] A.R. Levander, *Fourth-order finite-difference P-SV seismograms*, Geophysics, 53, pp 1425–1436, 1988.

[22] J. Lysmer and L.A. Drake, *A finite element method for seismology*, in B.A. Bolt, ed., Methods of Computational Physics, 11, Academic Press, New York, pp 181–216, 1972.

[23] R. Madariaga, *Dynamics of an expanding circular fault*, Bull. Seis. Soc. Am., 66, pp 639-666, 1976.

[24] K.J. Marfurt, *Accuracy of finite-difference and finite-element modelling of the scalar and elastic wave equations*, Geophysics, 49, pp 533–549, 1984.

[25] P. Moczo, E. Bystrický, J. Kristek, J.M. Carcione and M. Bouchon, *Hybrid modeling of P-SV seismic motion at inhomogeneous viscoelastic topographic structures*, Bull. Seism. Soc. Am., 87, pp 1305–1323, 1997.

[26] A. Pitarka, *3D elastic finite-difference modeling of seismic motion using staggered-grids with nonuniform spacing*, Bull. Seism. Soc. Am., 89, pp 85–106, 1999.

[27] W. Reed and T. Hill, *Triangular mesh methods for the neutron transport equation*, Technical Report LA-UR-73-479, Los Alamos Scientific Laboratory, Los Alamos, NM, 1973.

[28] C. Scheid and S. Lanteri, *Convergence of a Discontinuous Galerkin scheme for the mixed time domain Maxwell's equations in dispersive media*, INRIA report 7634, 2011.

[29] E.H. Saenger, N. Gold and S.A. Shapiro, *Modeling the propagation of elastic waves using a modified finite-difference grid*, Wave Motion, 31, pp 77–92, 2000.

[30] T. Bui-Thanh and O. Ghattas, *Analysis of an hp-nonconforming discontinuous Galerkin spectral element method for wave propagation*, SIAM J. Numer. Anal., 50(3), pp 1801–1826, 2012.

[31] J. Virieux, *P-SV wave propagation in heterogeneous media, velocity-stress finite difference method*, Geophysics, 51, pp 889–901, 1986.